Ab initio theory of the interlayer exchange coupling

Josef Kudrnovský[1,2], Václav Drchal[1,2], Ilja Turek[3,2], Patrick Bruno[4], Peter Dederichs[5], and Peter Weinberger[2]

[1] Institute of Physics, Academy of Sciences of the Czech Republic, CZ-182 21 Praha 8, Czech Republic
[2] Center for Computational Materials Science, Technical University, A-1060 Vienna, Austria
[3] Institute of Physics of Materials, Academy of Sciences of the Czech Republic, CZ-616 62 Brno, Czech Republic
[4] Max-Planck Institut für Mikrostrukturphysik, D-06120 Halle, Germany
[5] Institut für Festkörperforschung, Forschungszentrum Jülich, D-52425 Jülich, Germany

Abstract. *Ab initio* formulations of the interlayer exchange coupling (IEC) between two, in general non-collinearly aligned magnetic slabs embedded in a non-magnetic spacer are reviewed whereby both the spacer and the magnetic slabs as well as their interfaces may be either ideal or random. These formulations are based on the spin-polarized surface Green function technique within the tight-binding linear muffin-tin orbital method, the Lloyd formulation of the IEC, and the coherent potential approximation using the vertex-cancellation theorem. We also present an effective method for the study of the temperature dependence of the IEC. The periods, amplitudes, and phases are studied in terms of discrete Fourier transformations, the asymptotic behavior of the IEC is briefly discussed within the stationary-phase method. Numerical results illustrating the theory are presented.

1 Introduction

Oscillatory interlayer exchange coupling (IEC) has been found in a number of ferromagnetic/non-magnetic multilayer systems and is in some cases accompanied by an oscillatory magnetoresistance. The physical origin of such oscillations is attributed to quantum interferences due to spin-dependent confinement of the electrons in the spacer. The periods of the oscillations with respect to the spacer thickness can be correlated to the spacer Fermi surface, a relation frequently used in experimental studies. A number of models was proposed to explain this phenomenon and we refer the reader to excellent recent reviews on the subject[1,2,3].

The situation is much less satisfactory if the amplitudes and/or phases are concerned. They both depend sensitively on the details of the Fermi surface, and, from the experimental point of view, on the quality of the multilayers. Typically, samples include various amounts of disorder at interfaces as well

as in the bulk (e.g., surface roughness, intermixing, impurities, grain boundaries, etc.) which can influence the amplitudes and the phases significantly. From the theoretical standpoint of view it is important to keep in mind that the IEC is an oscillatory phenomenon for which, strictly speaking, amplitudes and/or phases are defined only in the asymptotic limit. Experimental data, however, are usually only available for the first few oscillations which are sufficient to extract periods, but not amplitudes and phases, in particular for the so-called long-period oscillations. The presence of impurities not only complicates the theoretical studies but also can provide a valuable insight into the effects controlling the IEC. In particular, substitutional alloying can provide a valuable informations concerning the topology of alloy Fermi surfaces. Alloying has also another, more subtle effect, namely it influences both amplitudes and phases and it can even introduce an extra damping of the oscillation amplitude (an exponential damping in addition to the usual $1/N^2$ decay, where N is the spacer thickness) if $\mathbf{k}_{\parallel}$-resolved electron states in the neighborhood of so-called callipers (extremal vectors of the Fermi surface) are influenced by disorder. Finally, we mention that a special case of alloying is intermixing of magnetic and spacer atoms at interfaces which can significantly influence coupling amplitudes and which occurs frequently during sample preparation in actual experiments.

It is thus obvious that the study of the effect of alloying on the periods, amplitudes, and phases of the IEC is an important issue which, however, is not properly reflected in the available literature. Conventional bandstructure methods are of limited use for such studies although in particular cases, when combined with the virtual-crystal-type approximations (VCA), they may be justified, e.g., for VCr or CrMn alloy spacers studied recently [4]. However, the complete neglect of alloy disorder makes a reliable determination of the coupling amplitudes or phases and, to some extent, even of the coupling periods, uncertain even in such favorable cases.

In addition, reliable conclusions and verifications of experimental measurements can only be based on a parameter-free theory. In order to determine the IEC one typically estimates the energy difference between the ferromagnetic (F) and antiferromagnetic (AF) alignment of a system consisting of two magnetic slabs separated by a non-magnetic spacer. Using total energy differences (evaluated with the local density approximation to the density functional theory) represents an extremely difficult task as the tiny exchange energies have to be subtracted from the background of huge total energies. Even if one employs very fast and accurate linear methods and computational tricks, the spacer thickness for which the calculated IEC values are reliable, is limited to about 20 layers [5,6]. On the other hand, for thin spacers this is the most accurate approach. One can alternatively employ asymptotic theories which are, strictly speaking, valid in the opposite regime, namely, for large spacer and magnetic slab thicknesses. The idea is to determine reflection (transmission) coefficients for an isolated interface between

magnetic and spacer metals and the extremal vectors of the spacer Fermi surface. The former quantities then determine the coupling amplitudes and phases while the latter quantities their periods. In this case the calculations can be performed by using conventional bandstructure methods and, in addition, they will provide a deep insight into the physical nature of the IEC [7]. Note, however, that neither of the above techniques can be extended to treat disorder nor can they be used to interpolate between two limits, namely, the case of thin spacers (preasymptotic region) and of thick spacers (asymptotic limit). For this a theory is needed which can bridge both the preasymptotic and the asymptotic region within a unified framework: IEC values for a large set of spacer thicknesses (say, for 1-100 atomic layers) can be analyzed in terms of discrete Fourier transformation in order to reliably determine not only periods, but also coupling amplitudes and phases. In addition, one can sample various subsets in order to analyze both the preasymptotic and the asymptotic regime as well as long-period oscillations.

The basic idea is to determine the IEC directly by employing the so-called magnetic force theorem [8,9] for rotations in spin space rather then shifting atoms as in the conventional force theorem [10]. We can thus use the same potentials for both the F and AF (or, in general, rotated) alignments of the magnetic slabs (the frozen-potential approximation) and consider only the single-particle (Kohn-Sham) energies.

This allows a direct formulation of interlayer exchange coupling based on an application of the Lloyd formula [11] in order to evaluate the difference between the grand canonical potentials of the F and AF alignment. The first calculations of that type were performed by Dederichs's group in Jülich [12]. The method used in the present paper extends the above approach in three relevant aspects: (i) a reformulation within the framework of a surface Green function technique by which linear scaling of the numerical effort with respect to the number of layers [13,14] is achieved; (ii) a proof of the so-called vertex-cancellation theorem [15] in order to study the influence of alloy disorder on the properties of the IEC, and (iii) an efficient method for a fast and accurate evaluation of integrals involving the Fermi-Dirac distribution function in order to study effects of finite temperature [16,17]. In the present paper we will review these particular techniques that were developed in the past few years and subsequently applied to a number of cases including alloy disorder [18,19,20,21,22]. In addition, we have studied systematically the effect of non-magnetic cap-layers [23,24] on the periods, the amplitudes, and the phases of the oscillations of the IEC.

2 Formalism

In this Section we derive an expression for the IEC for in general non-collinearly aligned magnetic slabs embedded in a non-magnetic spacer.

2.1 Geometry of the system

The system considered consists of a stack of layers, namely, from the left to the right: (i) a semi-infinite (nonmagnetic) substrate, (ii) a left ferromagnetic slab of thickness M (in monolayers, MLs), (iii) a nonmagnetic spacer of thickness N, (iv) a right ferromagnetic slab of thickness M', and (v) a semi-infinite (nonmagnetic) substrate. The thickness of the ferromagnetic slabs may extend to infinity. Eventually, one of the semi-infinite substrates may be substituted by a finite nonmagnetic cap of thickness P interfacing semi-infinite vacuum. In general, the various parts of the system can consist of different metals, including disordered substitutional alloys. We assume that the spin orientation of the right magnetic slab is rotated by an angle θ with respect to that of the left magnetic slab. In particular, the cases $\theta = 0$ and $\theta = \pi$ correspond to the ferromagnetic and antiferromagnetic alignments of magnetic moments of two subsystems, respectively.

2.2 Electronic structure of the system

The electronic structure of the multilayer is described by means of the tight-binding linear-muffin tin orbital (TB-LMTO) method [25]. In particular we employ the all-electron scalar-relativistic version as generalized to the case of random alloys, their surfaces and interfaces [26,27]. The key quantity of the formalism, the physical Green function $G(z)$, is expressed via the auxiliary Green function $g^{\alpha}(z)$ in the screened tight-binding LMTO representation α as

$$G(z) = \lambda^{\alpha}(z) + \mu^{\alpha}(z)\, g^{\alpha}(z)\, \mu^{\alpha}(z)\,, \tag{1}$$

where

$$g^{\alpha}(z) = \left(P^{\alpha}(z) - S^{\alpha}\right)^{-1}\,. \tag{2}$$

Here S^{α} is a matrix of screened structure constants $S^{\alpha}_{\mathbf{R}L,\mathbf{R}'L'}$, and $P^{\alpha}(z)$ is a site-diagonal matrix of potential functions $P^{\alpha,\sigma}_{\mathbf{R}L}(z)$. The potential functions are diagonal with respect to the angular momentum index $L = (\ell m)$ and the spin index $\sigma = \uparrow, \downarrow$ while the structure constants are spin-independent. The potential functions can be expressed via the so-called potential parameters C, Δ, and γ in the following manner

$$P^{\alpha}(z) = \frac{z - C}{\Delta + (\gamma - \alpha)(z - C)}\,, \tag{3}$$

where for matters of simplicity all indices are dropped. Similarly, the quantities λ^{α} and μ^{α} in (1) can be expressed as

$$\lambda^{\alpha}(z) = \frac{\gamma - \alpha}{\Delta + (\gamma - \alpha)(z - C)}\,, \quad \mu^{\alpha}(z) = \frac{\sqrt{\Delta}}{\Delta + (\gamma - \alpha)(z - C)}\,. \tag{4}$$

As only the screened representation will be used the superscript α is omitted in the following.

A separate problem is the determination of potential functions $P(z)$ for a given layered structure. Here we only mention that by employing the magnetic force theorem we can use the same potential functions for the ferromagnetic and rotated (or, antiferromagnetic) alignments. For random systems treated within the so-called coherent potential approximation (CPA) the potential function $P(z)$ is substituted by its coherent potential counterpart, $\mathcal{P}(z)$, whereby the formal structure of the Green function (2) remains the unchanged. The methods of determination of (coherent) potential functions for collinear alignments of magnetic moments in the present context can be found elsewhere [27,26].

2.3 Definition of the IEC

The exchange coupling energy $\mathcal{E}_x$, evaluated in the framework of the magnetic force theorem, is defined as the difference of the grand canonical potential Ω_λ between the ferromagnetic ($\lambda = F$) and antiferromagnetic ($\lambda = AF$) alignments of two subsystems, i.e. $\mathcal{E}_x = \Omega_{AF} - \Omega_F$. More generally, the quantity of the physical interest is the difference of the grand canonical potentials between a rotated ($\theta \neq 0$) and the ferromagnetic ($\theta = 0$) alignment of the two magnetic slabs, namely, $\mathcal{E}_x(\theta) \equiv \delta\Omega(\theta) = \Omega(\theta) - \Omega(0)$.

The grand canonical potential Ω of a system is defined by

$$\Omega(T,\mu) = -\int_{-\infty}^{\infty} f(E,T,\mu)\; N(E)\; \mathrm{d}E\,, \tag{5}$$

where $N(E)$ is the integrated valence density of states, $f(E,T,\mu)$ is the Fermi-Dirac distribution function at the temperature T and the chemical potential μ of electrons. It should be noted that at zero temperature the chemical potential coincides with the Fermi energy E_F of the system. The integrated valence density of states is then given by

$$N(E) = -\frac{1}{\pi}\,\mathrm{Im}\int_{-\infty}^{E} \mathrm{Tr}\, G(E'+i0)\;\mathrm{d}E'\,, \tag{6}$$

where Tr means the trace over lattice sites $\mathbf{R}$, angular momentum indices $L = (\ell m)$ and spin indices σ. Using (3,4), the following identities can be verified

$$\frac{d}{dz}\lambda(z) = -\lambda^2(z)\,, \quad \frac{d}{dz}P(z) = \mu^2(z)\,. \tag{7}$$

Together with formula (94), we find

$$\frac{d}{dz}\Big[\mathrm{Tr}\,\ln\lambda(z) + \mathrm{Tr}\,\ln g(z)\Big] = -\mathrm{Tr}\, G(z)\,. \tag{8}$$

The grandcanonical potential (5) is then expressed as

$$\Omega(T,\mu) = -\frac{1}{\pi}\,\mathrm{Im}\int_{-\infty}^{\infty} f(E,T,\mu)\;\mathrm{Tr}\ln\lambda(E+i0)\;\mathrm{d}E \\ -\frac{1}{\pi}\,\mathrm{Im}\int_{-\infty}^{\infty} f(E,T,\mu)\;\mathrm{Tr}\ln g(E+i0)\;\mathrm{d}E\,. \tag{9}$$

The formula in (9) is the expression for the grandcanonical potential within the TB-LMTO method [28] and for finite temperatures.

The rotated magnetic configuration is characterized by the set of rotation angles $\Theta = \{\theta_{\mathbf{R}}\}$ for all the lattice sites. In the reference (F) state all the angles $\theta_{\mathbf{R}} = 0$ while in the rotated state $\theta_{\mathbf{R}} = \theta$ in the rotated magnetic layer and $\theta_{\mathbf{R}} = 0$ for all other lattice sites. The quantities $\lambda(\Theta, z)$ and $g(\Theta, z)$ for the rotated system are given by

$$\lambda(\Theta,z) = \mathsf{U}(\Theta)\lambda(0,z)\mathsf{U}^{\dagger}(\Theta)\,,\;\; g(\Theta,z) = [\mathsf{U}(\Theta)P(0,z)\mathsf{U}^{\dagger}(\Theta) - S]^{-1}\,. \tag{10}$$

Here $[\mathsf{U}(\Theta)]_{\mathbf{R}\mathbf{R}'} = \delta_{\mathbf{R}\mathbf{R}'}U(\theta_{\mathbf{R}})$ is the rotation matrix for spin 1/2 particles defined in terms of the single-site matrices $U(\theta_{\mathbf{R}})$ [29]

$$\mathrm{U}(\theta) = \begin{pmatrix} c & s \\ -s & c \end{pmatrix}, \tag{11}$$

where $c = \cos(\theta/2)$, $s = \sin(\theta/2)$, $\mathrm{U}(\theta)\,\mathrm{U}^{\dagger}(\theta) = \mathrm{U}^{\dagger}(\theta)\,\mathrm{U}(\theta) = 1$, and $\mathrm{det}\mathrm{U}(\theta) = \mathrm{det}\mathrm{U}^{\dagger}(\theta) = 1$. We note that in the rotated magnetic configuration $P(\Theta, z) = \mathsf{U}(\Theta)P(0,z)\mathsf{U}^{\dagger}(\Theta)$ is generally a non-diagonal matrix with respect to the spin indices σ, σ'.

The first term in (9) is independent of θ because $\lambda(z)$ is site (and layer-) diagonal, it therefore does not contribute to the exchange energy $\mathcal{E}_x(\theta)$, i.e., it is sufficient to consider the second part only,

$$\Omega(\theta,T,\mu) = -\frac{1}{\pi}\,\mathrm{Im}\int_{-\infty}^{\infty} f(E,T,\mu)\;\mathrm{Tr}\ln g(\theta,E+i0)\;\mathrm{d}E\,. \tag{12}$$

It should be noted that the above expression is valid only in the absence of spin-orbit coupling.

The magnetic force theorem used here for the evaluation of the IEC was used also in related problems, e.g., for the evaluation of the exchange energies of two impurities embedded in a nonmagnetic host [8] and then extended to the case of Heisenberg exchange parameters between two sites in a magnetic material[9]. In the latter case the magnetic force theorem is valid only for the infinitesimal rotations while in the former case it is valid also for $\theta = \pi$ [30].

2.4 Configurational averaging

Keeping in mind applications to random systems, one is interested in the configurational average of the expression in (12), namely,

$$\langle\Omega\rangle = -\frac{1}{\pi}\,\mathrm{Im}\int_{-\infty}^{\infty} f(E,T,\mu)\;\langle\mathrm{Tr}\ln g(E+i0)\rangle\;\mathrm{d}E\,, \tag{13}$$

where $\langle \ldots \rangle$ denotes a configurational average. Difficulties here arise from the fact that the configurational average of the logarithm $\langle \ln g(z) \rangle$ can differ significantly from the logarithm of the configuration average $\ln \langle g(z) \rangle$. The difference $\mathsf{X} \equiv \langle \ln g \rangle - \ln \langle g \rangle$, the so-called vertex correction, is difficult to calculate and usually cannot be neglected. Fortunately, this problem can be circumvented by using the vertex cancellation theorem [15], which states that the contributions from the vertex correction for the F and AF configurations cancel each other exactly, namely $\mathrm{Tr}\ \mathsf{X}_{AF} - \mathrm{Tr}\ \mathsf{X}_F = 0$, such that to first order with respect to the angle between the magnetizations in the two ferromagnetic layers vertex corrections can be omitted. In other words, the evaluation of (13) simplifies to

$$\begin{aligned} \langle \Omega \rangle &= -\frac{1}{\pi} \,\mathrm{Im} \int_{-\infty}^{\infty} f(E,T,\mu)\ \mathrm{Tr} \ln \langle g(E+i0) \rangle \,\mathrm{d}E\,, \\ &= -\frac{1}{\pi} \,\mathrm{Im} \int_{C} f(z,T,\mu)\ \mathrm{Tr} \ln \langle g(z) \rangle \,\mathrm{d}z\,. \end{aligned} \tag{14}$$

We have also substituted the energy integral by integration over a contour in the complex energy plane z. The possibility to neglect vertex corrections can conveniently be used in calculations of the interlayer exchange coupling as explicit numerical calculations have shown that it remains valid to a good accuracy even for an angle as large as π [15]. In this respect it is very similar to the force theorem [10]. It is important to note that such an extension is only applicable to the evaluation of exchange energies of magnetic systems interacting via a non-magnetic host. An evaluation of exchange energies in ferromagnetic systems such as parameters of a classical Heisenberg model, was claimed to be limited to infinitesimal rotations only [9]. The use of the vertex-cancellation theorem allows to reduce the computational time in first-principles calculations by almost two orders of magnitude, so that the computational effort for disordered systems is comparable to that for a pure system [15]. We refer the reader to Appendix A for more details concerning the derivation and applicability of the vertex-cancellation theorem. The last remark concerns the fact that the expression for the change in the grandcanonical potential within the magnetic force theorem also includes the classical magnetostatic dipole-dipole interaction energy (DDIE). The DDIE decays with a spacer thickness much faster than the IEC and its contribution can be thus neglected for thicker spacer anyhow. In addition, first-principles fully-relativistic calculations of the IEC [32] have demonstrated that this term has a negligible influence even for a rather thin spacer amounting just to a few layers. Consequently, the DDIE term will be neglected in the following.

2.5 Lloyd formula

We need to evaluate the difference of configurationally averaged grandcanonical potentials in the rotated and FM configurations. This can be done conveniently with the help of the well-known Lloyd formula [11] applied to layered

systems. We formally split the system into two non-interacting fragments, namely a left fragment $\mathcal{L}$, which consists of the left substrate and the left magnetic slab, and a right fragment $\mathcal{R}$, which comprises the rest of the system, i.e., the spacer, the right magnetic slab, and the right substrate (or, eventually, the cap layer interfacing the vacuum). Fragments are described by the unperturbed Green function $\langle g_0(z)\rangle$. In the next step we couple two fragments together with help of a localized potential V which is simply the interlayer screened structure constant. This procedure has a number of advantages as compared to a conventional way of embedding two finite magnetic layers into the infinite (bulk) host spacer [12]: (i) the perturbation V is independent of the thicknesses of magnetic layers; (ii) complicated sample geometries can be treated, including semi-infinite magnetic layers; and (iii) a powerful and efficient method exists for the evaluation of the Green function of fragments, namely the surface Green function technique in the principal-layer formulation [26,27].

Keeping in mind the vertex cancellation theorem, one gets for a difference in the configurationally averaged grandcanonical potential (14), the expression

$$\langle \delta\Omega \rangle = -\frac{1}{\pi} \operatorname{Im} \int_C f(z,T,\mu)\, \operatorname{Tr} \ln\, (1 - V\, \langle g_0(z) \rangle)\, \mathrm{d}z\,, \tag{15}$$

where $\langle g_0(z)\rangle$ is the configurationally averaged Green function of the decoupled non-interacting fragments $\mathcal{L}$ and $\mathcal{R}$ defined above. For the sake of simplicity, we will denote from here on the configurationally averaged quantities by an overbar, e.g., $\langle g_0(z)\rangle \equiv \bar{g}_0(z)$. The concept of principal layers (PL) [33] as used within the TB-LMTO method leads to a block tridiagonal form of the structure constants and of the inverse Green function. If we apply this tridiagonality to (15), we get for V and $\langle g_0(z)\rangle$ the following expressions by using a supermatrix notation with respect to nearest-neighbor PLs resolved in the wave-vector $\mathbf{k}_\parallel$,

$$V(\mathbf{k}_\parallel) = \begin{pmatrix} 0 & S_{10}(\mathbf{k}_\parallel) \\ S_{01}(\mathbf{k}_\parallel) & 0 \end{pmatrix}\,,\;\; \bar{g}_0(\mathbf{k}_\parallel, z) = \begin{pmatrix} \bar{\mathcal{G}}_{\mathcal{L}}(\mathbf{k}_\parallel, z) & 0 \\ 0 & \bar{\mathcal{G}}_{\mathcal{R}}(\mathbf{k}_\parallel, z) \end{pmatrix}\,, \tag{16}$$

where $S_{10}(\mathbf{k}_\parallel) = \left[S_{01}(\mathbf{k}_\parallel)\right]^\dagger$. Combining (15) and (16) one gets

$$\delta \operatorname{Tr} \ln \bar{\mathcal{G}}(z) = -\frac{1}{N_\parallel} \sum_{\mathbf{k}_\parallel} \operatorname{tr} \ln\, \left[1 - \bar{\Gamma}_{\mathcal{L}}(\mathbf{k}_\parallel, z)\, \bar{\mathcal{G}}_{\mathcal{R}}(\mathbf{k}_\parallel, z)\right]\,, \tag{17}$$

$$\bar{\Gamma}_{\mathcal{L}}(\mathbf{k}_\parallel, z) = S_{10}(\mathbf{k}_\parallel)\, \bar{\mathcal{G}}_{\mathcal{L}}(\mathbf{k}_\parallel, z)\, S_{01}(\mathbf{k}_\parallel)\,.$$

Here the quantity $\bar{\Gamma}_{\mathcal{L}}(\mathbf{k}_\parallel, z)$ has the meaning of an effective embedding potential, and the quantities $\bar{\mathcal{G}}_{\mathcal{L}}$ and $\bar{\mathcal{G}}_{\mathcal{R}}$ are the configurationally averaged surface Green functions (SGF) [33] of the magnetic subsystems $\mathcal{L}$ and $\mathcal{R}$, respectively. By definition, the surface Green function $\bar{\mathcal{G}}_{\mathcal{S}}$ ($\mathcal{S} = \mathcal{L}, \mathcal{R}$) is the top PL projection of the Green function of the corresponding semi-infinite system $\mathcal{S}$.

Its determination in the case of random systems was extensively discussed in the literature, see [34,35,36,26]. The summation in (17) extends over the surface Brillouin zone (SBZ) corresponding to the underlying two-dimensional translational symmetry [37], and $N_\parallel$ is the number of sites in a layer.

2.6 The IEC for a general angle θ

Let us now turn to the evaluation of the energy difference between arbitrary alignments. Consider the following quantity,

$$\mathrm{tr}\ln \mathrm{Z} = \mathrm{tr}\ln\left(1 - \mathrm{A}_0\ \mathrm{B}\right) - \mathrm{tr}\ln\left(1 - \mathrm{A}_0\ \mathrm{B}_0\right), \tag{18}$$

where the matrices A_0 and B_0 are related to the ferromagnetic alignment and thus are diagonal in spin space

$$\mathrm{A}_0 = \begin{pmatrix} \mathrm{A}_0^{\uparrow} & 0 \\ 0 & \mathrm{A}_0^{\downarrow} \end{pmatrix}, \quad \mathrm{B}_0 = \begin{pmatrix} \mathrm{B}_0^{\uparrow} & 0 \\ 0 & \mathrm{B}_0^{\downarrow} \end{pmatrix}. \tag{19}$$

The particular form of the subblocks A_0^σ and B_0^σ ($\sigma = \uparrow, \downarrow$) is given by

$$\mathrm{A}_0^\sigma = S_{10}(\mathbf{k}_\parallel)\,\bar{\mathcal{G}}_{\mathcal{L}}^\sigma(\mathbf{k}_\parallel, z)\,S_{01}(\mathbf{k}_\parallel), \qquad \mathrm{B}_0^\sigma = \bar{\mathcal{G}}_{\mathcal{R}}^\sigma(\mathbf{k}_\parallel, z). \tag{20}$$

The matrix B refers to an alignment in which the orientations of the magnetization in two magnetic slabs are rotated uniformly by a relative angle θ,

$$\mathrm{B} = \mathrm{U}(\theta)\,\mathrm{B}_0\,\mathrm{U}^\dagger(\theta), \tag{21}$$

where $\mathrm{U}(\theta)$ is the rotation matrix (11). The quantity $1 - \mathrm{A}_0\,\mathrm{B}$ in (18) can therefore be written as

$$1 - \mathrm{A}_0\ \mathrm{B} = \Big(\mathrm{U}(\theta) - \mathrm{A}_0\mathrm{U}(\theta)\mathrm{B}_0\Big)\mathrm{U}^\dagger(\theta), \tag{22}$$

where, as follows from (19) and (11),

$$\mathrm{U}(\theta) - \mathrm{A}_0\ \mathrm{U}(\theta)\ \mathrm{B}_0 = \begin{pmatrix} c\ (1 - \mathrm{A}_0^{\uparrow}\ \mathrm{B}_0^{\uparrow}) & s\ (1 - \mathrm{A}_0^{\uparrow}\ \mathrm{B}_0^{\downarrow}) \\ -s\ (1 - \mathrm{A}_0^{\downarrow}\ \mathrm{B}_0^{\uparrow}) & c\ (1 - \mathrm{A}_0^{\downarrow}\ \mathrm{B}_0^{\downarrow}) \end{pmatrix}. \tag{23}$$

Using now the identity $\mathrm{tr}\ln\,\mathrm{X} = \ln\det\,\mathrm{X}$, which is valid for any non-singular matrix X, and the identity

$$\det\begin{pmatrix} \mathrm{A} & \mathrm{B} \\ \mathrm{C} & \mathrm{D} \end{pmatrix} = \det\mathrm{A}\,.\,\det\mathrm{D}\,.\,\det(1 - \mathrm{A}^{-1}\,\mathrm{B}\,\mathrm{D}^{-1}\,\mathrm{C}), \tag{24}$$

which in turn is valid, if the matrices A and D are non-singular, it is straightforward to prove that

$$\mathrm{tr}\ln\ \mathrm{Z} = \mathrm{tr}_L\ln\left(1 - \frac{1 - \cos(\theta)}{2}\,\mathrm{M}\right), \tag{25}$$

where

$$\mathrm{M} = 1 - (1 - \mathrm{A}_0^{\uparrow}\,\mathrm{B}_0^{\uparrow})^{-1}\,(1 - \mathrm{A}_0^{\uparrow}\,\mathrm{B}_0^{\downarrow})\,(1 - \mathrm{A}_0^{\downarrow}\,\mathrm{B}_0^{\downarrow})^{-1}\,(1 - \mathrm{A}_0^{\downarrow}\,\mathrm{B}_0^{\uparrow})\,. \tag{26}$$

It should be noted that in (18) tr denotes the trace over angular momenta and spin, while in (24) tr_L denotes the trace over orbital momenta only. The final expression for $\mathcal{E}_x(\theta)$ is thus given by

$$\mathcal{E}_x(\theta) = \frac{1}{\pi N_{\parallel}} \sum_{\mathbf{k}_{\parallel}} \mathrm{Im} \int_C f(z,T,\mu) \times \mathrm{tr}_L \ln \left(1 - \frac{1-\cos(\theta)}{2}\,\mathrm{M}(\mathbf{k}_{\parallel},z)\right) \mathrm{d}z\,, \tag{27}$$

in which the energy integral is expressed in terms of a contour integral which will be discussed in detail later.

It is interesting to note that the expression (26) for $\mathrm{M}(\mathbf{k}_{\parallel},z)$ can be rearranged in the following form [19]

$$\mathrm{M} = -\,\left(1 - S_{10}\,\bar{\mathcal{G}}_{\mathcal{L}}^{\uparrow}\,S_{01}\,\bar{\mathcal{G}}_{\mathcal{R}}^{\uparrow}\right)^{-1} S_{10}\left(\bar{\mathcal{G}}_{\mathcal{L}}^{\uparrow} - \bar{\mathcal{G}}_{\mathcal{L}}^{\downarrow}\right) \times \left(1 - S_{01}\,\bar{\mathcal{G}}_{\mathcal{R}}^{\downarrow}\,S_{10}\,\bar{\mathcal{G}}_{\mathcal{L}}^{\downarrow}\right)^{-1} S_{01}\left(\bar{\mathcal{G}}_{\mathcal{R}}^{\uparrow} - \bar{\mathcal{G}}_{\mathcal{R}}^{\downarrow}\right)\,. \tag{28}$$

It explicitly factorizes the 'spin-asymmetry' of the problem and it is directly related to RKKY-like theories [1]. This result [19] is formally equivalent to the results of the spin current approach [39] as formulated within a Green function formalism based on an empirical single orbital tight-binding model [40]. A matrix version developed in the framework of a semiempirical tight-binding model has appeared recently [2].

For completeness we also give the result for the common case of the antiferromagnetic alignment ($\theta = \pi$):

$$\mathcal{E}_x \equiv \mathcal{E}_x(\pi) = \frac{1}{\pi N_{\parallel}} \sum_{\mathbf{k}_{\parallel}} \mathrm{Im} \int_C f(z,T,\mu)\ \mathrm{tr}_L \ln \mathcal{M}(\mathbf{k}_{\parallel},z)\,\mathrm{d}z\,, \tag{29}$$

where $\mathcal{M}$ is a product of four terms,

$$\mathcal{M} = (1 - \mathrm{A}_0^{\uparrow}\,\mathrm{B}_0^{\uparrow})^{-1}\,(1 - \mathrm{A}_0^{\uparrow}\,\mathrm{B}_0^{\downarrow})\,(1 - \mathrm{A}_0^{\downarrow}\,\mathrm{B}_0^{\downarrow})^{-1}\,(1 - \mathrm{A}_0^{\downarrow}\,\mathrm{B}_0^{\uparrow})\,. \tag{30}$$

2.7 The torque and infinitesimal rotations

The differential change in the grand canonical potential $\delta\Omega(\theta)$ with respect to a differential relative angle θ, $-\partial\,\delta\Omega(\theta)/\partial\,\theta$, is usually called the torque. The torque can easily be obtained by differentiating (27) with respect to the angle θ. By definition one gets therefore

$$T(\theta) = -\frac{\partial \mathcal{E}_x(\theta)}{\partial\theta} \qquad \text{or} \qquad \mathcal{E}_x(\theta) = -\int_0^{\theta} T(\theta')\,d\theta'\,, \tag{31}$$

whereby $T(\theta)$ follows immediately from (27)

$$T(\theta) = \frac{\sin(\theta)}{2\pi N_\parallel} \sum_{\mathbf{k}_\parallel} \mathrm{Im} \int_C f(z,T,\mu) \times \mathrm{tr}_L \left[\mathrm{M}(\mathbf{k}_\parallel, z) \left(1 - \frac{1}{2} \left[1 - \cos(\theta) \right] \mathrm{M}(\mathbf{k}_\parallel, z) \right)^{-1} \right] \mathrm{d}z \,. \quad (32)$$

By formally expanding the logarithm in (27) in powers of $1 - \cos(\theta)$, one can cast the expression for $\mathcal{E}_x(\theta)$ into the form

$$\mathcal{E}_x(\theta) = B_1 \left[1 - \cos(\theta) \right] + \frac{1}{2} B_2 \left[1 - \cos(\theta) \right]^2 + \ldots \,, \quad (33)$$

where B_1 and B_2 are the so-called bilinear and the (intrinsic) biquadratic exchange coupling coefficients, respectively,

$$B_1 = \frac{1}{2\pi N_\parallel} \sum_{\mathbf{k}_\parallel} \mathrm{Im} \int_C f(z,T,\mu)\, \mathrm{tr}_L\, \mathrm{M}(\mathbf{k}_\parallel, z)\, \mathrm{d}z \,, \quad (34)$$

$$B_2 = -\frac{1}{4\pi\, N_\parallel} \sum_{\mathbf{k}_\parallel} \mathrm{Im} \int_C f(z,T,\mu)\, \mathrm{tr}_L\, \left[\mathrm{M}(\mathbf{k}_\parallel, z) \right]^2 \mathrm{d}z \,.$$

It may be, however, more convenient to fit the exact expression (27) into the form (33) by employing calculated values for $\theta = \pi/2$ and $\theta = \pi$ [41]. We obtain

$$B_1 = \frac{\mathcal{E}_x(\pi) + 2\mathcal{E}_x(\pi/2)}{2} \,, \qquad B_2 = \frac{\mathcal{E}_x(\pi) - 2\mathcal{E}_x(\pi/2)}{2} \,. \quad (35)$$

Of particular interest is the expansion of $\mathcal{E}_x(\theta)$ for a small θ, i.e., when $1 - \cos(\theta)$ is a small parameter (the method of infinitesimal rotations (MIR)). This approach becomes particularly relevant in the case when the spacer is a magnetic metal or for complicated geometries, e.g., for so-called periodic multilayers.

2.8 The IEC as interface-interface interaction

We will now discuss briefly an alternative approach of a direct evaluation of the IEC as a difference in the interface-interface interaction energies rather then its indirect determination in terms of the energy of a single interface (13-16). We decouple the system into three fragments, a left, central, and right fragment, $\mathcal{L}$, $\mathcal{C}$, and $\mathcal{R}$, respectively. The left and the right fragment are formed by corresponding substrates with magnetic slabs whereby the central slab comprises the spacer. Both approaches are physically equivalent because it is irrelevant how the system is divided into an unperturbed part and a perturbation. Note, however, that the interface-interface formulation is more

general as it could be used for a determination of interaction energies of two generally different interfaces.

The derivation proceeds in two steps and employs partitioning technique with respect to the trace of the logarithm of the Green function. First, the subsystems $\mathcal{L}$ and $\mathcal{R}$ are downfolded which leads to an effective problem of two localized perturbations in the subsystem $\mathcal{C}$. The second step, a two-potential formula applied to the fragment $\mathcal{C}$ separates directly the interface-interface contribution. The result has formally the same structure as the previous one (17,26), but the subblocks A_0^σ and B_0^σ ($\sigma =\uparrow,\downarrow$) are now of the following form

$$\mathrm{A}_0^\sigma = \bar{g}_{N1}(\mathbf{k}_\parallel, z)\, \bar{\tau}_1^\sigma(\mathbf{k}_\parallel, z)\, \bar{g}_{1N}(\mathbf{k}_\parallel, z)\,, \qquad \mathrm{B}_0^\sigma = \bar{\tau}_N^\sigma(\mathbf{k}_\parallel, z)\,. \tag{36}$$

The τ-matrices $\bar{\tau}_i$ ($i = 1, N$) corresponding to "multiple scattering" at individual interfaces $\mathcal{L}/\mathcal{C}$, ($i = 1$) and $\mathcal{C}/\mathcal{R}$, ($i = N$) are expressed as

$$\bar{\tau}_i^\sigma(\mathbf{k}_\parallel, z) = \bar{\Gamma}_i^\sigma(\mathbf{k}_\parallel, z)\, \left[1 - \bar{g}_{ii}(\mathbf{k}_\parallel, z)\, \bar{\Gamma}_i^\sigma(\mathbf{k}_\parallel, z)\right]^{-1}\,, \tag{37}$$

where the effective embedding potentials $\bar{\Gamma}_i^\sigma(\mathbf{k}_\parallel, z)$ of the left and right interfaces ($i = 1, N$), respectively, are defined as

$$\begin{aligned} \bar{\Gamma}_1^\sigma(\mathbf{k}_\parallel, z) &= S_{10}(\mathbf{k}_\parallel)\, \bar{\mathcal{G}}_{\mathcal{L}}^\sigma(\mathbf{k}_\parallel, z)\, S_{01}(\mathbf{k}_\parallel)\,, \\ \bar{\Gamma}_N^\sigma(\mathbf{k}_\parallel, z) &= S_{01}(\mathbf{k}_\parallel)\, \bar{\mathcal{G}}_{\mathcal{R}}^\sigma(\mathbf{k}_\parallel, z)\, S_{10}(\mathbf{k}_\parallel)\,. \end{aligned} \tag{38}$$

Here, $\bar{\mathcal{G}}_{\mathcal{S}}^\sigma$ ($\mathcal{S} = \mathcal{L}, \mathcal{R}$) are the configurationally averaged SGFs of the left and the right semi-infinite regions, respectively. Details of the derivation can be found in Appendices B and C. The coupling between the two magnetic subsystems is due to the layer off-diagonal projections $\bar{g}_{1N}(\mathbf{k}_\parallel, z)$ and $\bar{g}_{N1}(\mathbf{k}_\parallel, z)$ of the Green function (GF) of the finite spacer consisting of N layers. The oscillatory behavior of interlayer coupling is then governed by the oscillatory behavior of these quasi one-dimensional spacer Green functions, a formulation which is very much in the spirit of a simplified RKKY approach [1]. An efficient method of evaluation of the corner-blocks of the Green function, $\bar{g}_{ij}(\mathbf{k}_\parallel, z)$, ($i, j = 1, N$), is described in Appendix D [42,36].

2.9 Relation to the KKR method

We shall discuss now the relation of the present approach (29,30,36) to the method employed in [12] and based on the Korringa-Kohn-Rostoker (KKR) Green function technique. Let us note first the deep internal connection between the KKR and the TB-LMTO-GF approach (see [26,43] for more details). The model in (12) consists of an infinite ideal non-magnetic spacer as a reference system and of two magnetic slabs representing localized perturbations. For simplicity we start from the case of two magnetic monolayers in an infinite spacer. The result

$$\mathrm{A}_0^\sigma = \mathcal{G}_{N1}^b(z)(\mathbf{k}_\parallel, z)\, t_1^\sigma(\mathbf{k}_\parallel, z)\, \mathcal{G}_{1N}^b(\mathbf{k}_\parallel, z)\,, \qquad \mathrm{B}_0^\sigma = t_N^\sigma(\mathbf{k}_\parallel, z) \tag{39}$$

is formally the same with the exception that the τ-matrices entering (36) are now substituted by the single-site t-matrices t_i which describe the scattering of electrons from two magnetic monolayers at $i = 1, N$ embedded in an infinite non-random bulk spacer and separated by $N - 2$ spacer layers:

$$t^{\sigma}_{\lambda;\,i}(\mathbf{k}_{\parallel}, z) = \Delta P^{\sigma}_{\lambda;\,i}(z)\ \left[1 + \mathcal{G}^{b}(\mathbf{k}_{\parallel}, z)\,\Delta P^{\sigma}_{\lambda;\,i}(z)\right]^{-1}\ . \tag{40}$$

The strength of the scattering potential, $\Delta P^{\sigma}_{\lambda;\,i}(z)$, is given by the difference of the potential functions for the magnetic monolayer $P^{\sigma}_{\lambda;\,i}(z)$ and for the non-magnetic spacer $P(z)$, while $\mathcal{G}^{b}(\mathbf{k}_{\parallel}, z)$ is the layer diagonal block of the GF of the bulk spacer. The layer off-diagonal blocks of the bulk spacer GF, $\mathcal{G}^{b}_{1N}(z)$ and $\mathcal{G}^{b}_{N1}(z)$, are given by

$$\mathcal{G}^{b}_{1N}(\mathbf{k}_{\parallel}, z) = \left[\mathcal{G}^{s}(\mathbf{k}_{\parallel}, z)\,S_{01}(\mathbf{k}_{\parallel})\right]^{N-1}\ \mathcal{G}^{b}(\mathbf{k}_{\parallel}, z)\,, \tag{41}$$

and similarly for $\mathcal{G}^{b}_{N1}(z)$. Here, $\mathcal{G}^{s}(\mathbf{k}_{\parallel}, z)$ is the corresponding SGF of an ideal semi-infinite non-magnetic bulk spacer [33]. It should be noted that also the layer-resolved bulk Green function $\mathcal{G}^{b}(\mathbf{k}_{\parallel}, z)$ can be expressed in terms of the SGFs (see, e.g., [34]). Since (41) is exact, there is no need to perform an additional $k_{\perp}$-integration [12]. It is easy to show that the result is formally identical to the case of two impurities in a simple tight-binding linear chain model with nearest neighbor hopping.

A generalization to the case of magnetic slabs containing a finite number M of magnetic layers is formally straightforward [12]. The t-matrices $t^{\sigma}_{\lambda;i}(z)$ are then supermatrices with respect to angular momentum and layer indices and the numerical effort to evaluate (40) increases with the third power of M as contrasted with the results of the present approach (17,36) which depend only linearly on M.

2.10 Influence of external periodicity

Until now it was assumed implicitly that we have a simple "parent" lattice [37]. The periods of the coupling oscillations are closely related to the Fermi surface geometry [1,2] of the bulk spacer. A different translational symmetry (complex lattices) or stacking sequence within layers will thus tend for sufficiently thick spacers to a different kind of bulk periodicity and hence to new periods. For example, an alternating stacking of fcc(001)-layers Cu and ordered c(2×2)-CuAu layers tends to an ordered fcc-Cu_3Au alloy with a Fermi surface topology different from that of fcc-Cu spacer. For a discussion of "superlattice" formation in magnetic multilayers see also [38]. We will discuss in the following in some detail two possibilities, namely superstructures in the spacer and in the magnetic slabs.

We start with the former case by assuming the same geometry as discussed in Sec. 2.1 but now the spacer slab consists of two non-magnetic metals A and B with respective thickness n_A and n_B periodically alternating. Typically, the spacer layer starts with the layer $A(B)$ and ends with the layer $B(A)$,

but the termination of the spacer slab with the same layers is also possible (and interesting [22]). The particular case of $n_A = n_B = 1$ corresponding to an (001)-stacking of an ordered fcc-CuAu alloy was already treated on a first-principles level [22]. The more general case, $(n_A, n_B > 1)$, which corresponds to artificially grown superstructures, was treated only within a simple one-band model [44]. In both cases, new periodicities (in comparison with the spacers consisting from pure A or B metals) arise with an increasing number of repetitions. Alternatively, one can consider a superstructure within a given spacer layer, or combination of both, e.g., the above mentioned example of the ordered fcc-Cu_3Au alloy spacer. The similar situation can be encountered also in the magnetic slabs. In particular the case of a c(2×2)-CoFe periodicity within the magnetic layers separated by a fcc-Cu(001) spacer [20] leads to the rather surprising appearance of new periods. These new periods can be now correlated to critical points of the spacer Fermi surface folded down to the Brillouin zone corresponding to a c(2×2)-superlattice [20]. A correlated gradual appearance of new periods and the order in statistically disordered layers is a clear indication of their relation to a different bulk periodicity [20,22].

A special case of alternating layers of A and B metals is when one of metals is magnetic and the other is nonmagnetic, all of which sandwiched between two substrates. This is the case of a periodic multilayer.

The generalization of the present formalism to above discussed cases is rather straightforward. In the case of a superlattice within a layer it is just sufficient to substitute matrices appearing in (27,29) by the corresponding supermatrices, e.g., by (2×2)-supermatrices in the case of a c(2×2)-superlattice. The key quantity, the surface Green functions $\bar{\mathcal{G}}^{\sigma}_{\mathcal{L},\mathcal{R}}$ (20), can be easily evaluated also in this case (see for details [26]). The generalization of the formalism to the case of alternating layers from A and B metals is as well simple because the surface Green function is constructed in an epitaxial manner, i.e., layer by layer, and it is therefore immaterial if the stacking of layers consists of the same or a different material. In the limit of a periodic multilayer we should just keep in mind that a proper repeating unit consists now from four layers, namely $S - M - S - M$, where the symbols S and M refer to the spacer and magnetic layers, respectively. This is necessary to calculate the F and AF configurations needed for the evaluation of the IEC. We note that the present formalism allows to evaluate efficiently and reliably the IEC for thick spacers (one hundred layers and more) which is important for realistic studies of so-called superlattice spacers and of periodic multilayers.

2.11 Temperature-dependence of the IEC

We conclude this Section by reviewing a recently developed technique for an efficient evaluation of the temperature dependence of the IEC [16]. The main cause for the temperature dependence of the IEC is connected with thermal excitations of electron-hole pairs across the Fermi level as described by the

Fermi-Dirac function. It turns out that other mechanisms (as for example electron-phonon and electron-magnon interactions) are less important. We rewrite (29) into the following form

$$\mathcal{E}_x(T) = \operatorname{Im} I(T)\,, \quad I(T) = \int_C f(z,T,\mu)\,\Psi(z)\,\mathrm{d}z\,, \tag{42}$$

where

$$\Psi(z) = \frac{1}{\pi N_\parallel} \sum_{\mathbf{k}_\parallel} \operatorname{tr}_L \ln \mathcal{M}(\mathbf{k}_\parallel, z)\,, \tag{43}$$

with the energy integration performed over a contour C along the real axis and closed by a large semicircle in the upper half of the complex energy plane.

The integral in (42) can be recast into a more suitable form using the analytic properties of $\Psi(z)$, namely, (i) $\Psi(z)$ is holomorphic in the upper half of the complex halfplane, and (ii) $z\Psi(z) \to 0$ for $z \to \infty$, $\mathrm{Im} z > 0$. Let us define a new function $\Phi(y) = -i\,\Psi(E_F + iy)$ of a real variable y, $y \geq 0$. Then at $T = 0$ K,

$$I(0) = \int_0^{+\infty} \Phi(y)\,\mathrm{d}y\,, \tag{44}$$

while at $T > 0$ K,

$$I(T) = 2\pi k_B T \sum_{k=1}^{\infty} \Phi(y_k)\,, \tag{45}$$

where k_B is the Boltzmann constant and the y_k are Matsubara energies, $y_k = \pi k_B T(2k-1)$. In the limit $T \to 0$, $I(T) \to I(0)$ continuously.

We have verified that the function $\Phi(y)$ can be represented accurately as a sum of a few complex exponentials of the form

$$\Phi(y) = \sum_{j=1}^{M} A_j \exp(p_j y)\,, \tag{46}$$

where the A_j are complex amplitudes and the p_j are complex wave numbers. An efficient method of finding the parameters A_j and p_j is described elsewhere [16]. The evaluation of $I(T)$ is then straightforward:

$$I(T) = -2\pi k_B T \sum_{j=1}^{M} \frac{A_j}{\exp(\pi k_B T p_j) - \exp(-\pi k_B T p_j)}\,, \tag{47}$$

which for $T = 0$ K gives

$$I(0) = -\sum_{j=1}^{M} \frac{A_j}{p_j}\,. \tag{48}$$

The efficiency of the present approach allows to perform calculations with a large number of $\mathbf{k}_\parallel$-points in the irreducible part of the surface Brillouin zone (ISBZ) in order to obtain accurate and reliable results. Note also that such calculations have to be done only once and then the evaluation of the IEC for any reasonable temperature is an easy task.

The effect of finite temperatures on the IEC can be evaluated also analytically. The analytical approach assumes the limit of large spacer thickness, for which all the oscillatory contributions to the energy integral cancel out with exception of those at the Fermi energy. The energy integral is then evaluated by a standard saddle-point method [1]. The general functional form of the temperature-dependence of the interlayer exchange coupling $\mathcal{E}_x(T)$ in the limit of a single period is then given by

$$\mathcal{E}_x(T) = \mathcal{E}_x(0)\, t(N,T)\,, \quad t(N,T) = \frac{cNT}{\sinh(cNT)}\,. \tag{49}$$

Here, N denotes the spacer thickness in monolayers, and c is a constant which depends on the spacer Fermi surface. The term $\mathcal{E}_x(0)$ exhibits a standard N^{-2}-dependence [1], while the scaling factor $t(N,T)$ depends on the product N and T. In the preasymptotic regime (small spacer thickness) the functional form of $t(N,T)$ differs from that of (49), particularly in the case of a complete, but relatively weak confinement due to the rapid variation of the phase of the integrand which enters the expression for the IEC [45]. The present numerical technique is free of the above discussed limitations and can be used to check conclusions of model theories.

3 Numerical results and discussion

3.1 Details of calculations

Special care has to be devoted to the energy and the Brillouin zone integrations. For a finite temperature we determine the parameters of the complex exponentials in (46) through an evaluation of $\Phi(y)$ at 40 Matsubara energies corresponding to $T = 25$ K. We have verified that the results depend weakly on the actual value of the parameter T. For $T = 0$ K we have tested two energy contours C, namely a semicircle between the bottom of the band (E_{min}) and E_F, or, alternatively, a line contour $E_F + i\,\varepsilon$, $\varepsilon \in (0, \infty)$, using a Gaussian quadrature. The results were very similar in both cases. Using a line contour avoids possible problems connected with the phase of a complex logarithm. Typically a total of 10-15 energy points was used. A large number of $\mathbf{k}_\parallel$-points in the ISBZ is needed only for energy points close to the real axis, whereby generally a greater number is needed for lower temperatures and thicker spacers. The number of $\mathbf{k}_\parallel$-points can significantly be reduced for energies well off the real axis. In particular, for the first energy point on the contour close to the Fermi energy we typically use 5000-10000 $\mathbf{k}_\parallel$-points

in the ISBZ, while for the next 3-4 energy points the number of $\mathbf{k}_\parallel$-points is reduced by a factor two for each other point, and about 50-100 $\mathbf{k}_\parallel$-points are taken for all remaining energy points on the contour. The thickness of the spacer, for which well converged results are obtained, is about 100 spacer layers.

3.2 Analysis of the results

The calculated results, namely $\mathcal{E}_x(\theta, N)$, where N specifies the spacer thickness, can be analyzed in terms of a discrete Fourier transformation

$$F(\theta, q) = \frac{1}{p} \sum_{N=N_{min}}^{N_{max}} N^2 \mathcal{E}_x(\theta, N) \, \exp(iqN) \,, \tag{50}$$

where $p = N_{max} - N_{min} + 1$ is the number of values used in the Fourier analysis, and N_{min} is chosen in order to eliminate the effect of very thin spacers, or, to analyze intentionally either the preasymptotic or the asymptotic region. Typically p is about 40. The background oscillations thus occurring [14] are due to the discreteness of the Fourier transformation. The background oscillations can be smoothened using the procedure described in [46], namely by multiplying $N^2\mathcal{E}_x(\theta, N)$ by $C \sin(\pi N/p)/(\pi N/p)$, where C is a normalization factor. The periods of oscillations Λ_α (in monolayers) are then identified with the positions q_α of pronounced peaks of $|F(q_\alpha)|$ as $\Lambda_\alpha = 2\pi/q_\alpha$, the amplitudes of oscillations A_α are estimated from $A_\alpha = (2/p)|F(q_\alpha)|$, and their phases from $\phi_\alpha = \pi/2 - \mathrm{Arg}F(q_\alpha)$, $(\alpha = 1, 2, \ldots)$. This analysis can be extended to more complicated cases, namely when the IEC is a function of two variables, e.g., as a function of the spacer and cap thicknesses N and P, respectively. A two-dimensional discrete Fourier transformation

$$F_2(\theta, q_N, q_P) = \sum_{N=N_1}^{N_2} \sum_{P=P_1}^{P_2} (N+P)^2 \, \mathcal{E}_2(\theta, N, P) \, \mathrm{e}^{\mathrm{i}(q_N N + q_P P)} \tag{51}$$

is a suitable tool to analyze the quantity $\mathcal{E}_2(\theta, N, P)$, where the prefactor $(N+P)^2$ is consistent with the asymptotic behavior [23,47] for large spacer and cap thickness. Strictly speaking, this is quite an obvious choice for the case when the spacer and cap are formed by the same material, but it can be used also when the spacer and the cap correspond to different materials (for more details, see [23]). In (51) we have introduced the quantity

$$\mathcal{E}_2(\theta, N, P) = \mathcal{E}_x(\theta, N, P) - \mathcal{E}_0(\theta, N) \,, \quad \mathcal{E}_0(\theta, N) = \lim_{P \to \infty} \mathcal{E}_x(\theta, N, P) \tag{52}$$

in order to remove a trivial peak in the absolute value of $F_2(\theta, q_N, q_P)$ at $q_N = q_P = 0$. A similar two-dimensional discrete Fourier transformation is also useful in the study of the IEC with respect to the thicknesses of the spacer and the magnetic slabs. We note that if one of variables, e.g., the spacer

thickness N is fixed, it is possible to analyze the calculated IEC values again with the help of (50).

An alternative of calculating the Fourier transform (50) consists in subdividing the $\mathbf{k}_\parallel$-integral in (27) into areas around the critical $\mathbf{k}_\parallel$-vectors (callipers) related to the different oscillation periods [30,49]. In the asymptotic limit each subarea gives then rise to a single oscillation period, while in the preasymptotic regime the resulting division into different periods is only qualitatively valid. In a sense this method bridges the present method of discrete Fourier transformations and the purely asymptotic treatment of calculating only the behavior of the critical $\mathbf{k}_\parallel$-vectors (see Section 3.3).

3.3 Asymptotic expansion

Model studies [1,2] indicate that in the asymptotic region, i.e., for large spacer and magnetic layer thickness, and for a random sample, the general form of the spacer-thickness dependence of the IEC is given by

$$\mathcal{E}_x = \mathrm{Im} \sum_\alpha \frac{Z_\alpha}{N^2} \exp(iQ_\alpha N)\,. \tag{53}$$

Here the sum runs over all possible periods α, the quantities Z_α and Q_α are the complex amplitudes and complex stationary points (callipers), respectively, defined in the following manner

$$Z_\alpha = A_\alpha \exp(i\Phi_\alpha)\,, \qquad Q_\alpha = q_\alpha + i\lambda_\alpha\,. \tag{54}$$

The quantities A_α and Φ_α are the amplitudes and phases of coupling oscillations, $p_\alpha = 2\pi/q_\alpha$ their periods, and the quantity λ_α characterizes the damping of oscillations due to the effect of alloying in the sample determined at the Fermi energy. In the limit of non-random samples, $\lambda_\alpha = 0$.

The parameters in (53) can be extracted from a detailed knowledge of the spacer Fermi surface [7]. We briefly sketch a numerical way of determining of the parameters of this asymptotic expansion which requires the knowledge of the integrand of (29) for a set of $\mathbf{k}_\parallel$-points in the neighborhood of the stationary points $\mathbf{k}_\parallel^{(\alpha)}$.

The expression (29) for IEC at $T = 0$ K can be rewritten as

$$\mathcal{E}_x = \frac{1}{N_\parallel} \mathrm{Im} \sum_{\mathbf{k}_\parallel} Y(\mathbf{k}_\parallel)\,, \;\; Y(\mathbf{k}_\parallel) = \frac{1}{\pi} \int_C f(z,0)\, \mathrm{tr}_L \, \ln \mathcal{M}(\mathbf{k}_\parallel, z)\, \mathrm{d}z\,. \tag{55}$$

The integration with respect to the energy variable is performed numerically. The function $Y(\mathbf{k}_\parallel)$ for large N decreases as $O(1/N)$ and behaves like

$$Y(\mathbf{k}_\parallel) = \frac{g(\mathbf{k}_\parallel)}{N} \exp(iN\phi(\mathbf{k}_\parallel))\,, \tag{56}$$

where the pre-exponential factor $g(\mathbf{k}_\parallel)$ is a smooth function of $\mathbf{k}_\parallel$ and the phase $\phi(\mathbf{k}_\parallel)$ has one, or more stationary points in the SBZ that correspond

to callipers of the spacer Fermi surface such that $\nabla_{\mathbf{k}_\parallel}\phi(\mathbf{k}_\parallel)=0$. The integral over the SBZ in (55) can be evaluated using the stationary-phase method. The contribution of a stationary point $\mathbf{k}_\parallel^{(\alpha)} \equiv (k_x^{(\alpha)}, k_y^{(\alpha)})$ is found in the following way: the integration limits are extended to infinity, and the phase function $\phi(\mathbf{k}_\parallel)$ is approximated by a quadratic function of $\mathbf{k}_\parallel \equiv (k_x, k_y)$ in the vicinity of the stationary point,

$$\begin{aligned}\phi(\mathbf{k}_\parallel) &= \phi(\mathbf{k}_\parallel^{(\alpha)}) + \sum_{i,j=x,y} Q_{ij}(k_i - k_i^{(\alpha)})(k_j - k_j^{(\alpha)}) \\ &= \sum_{i,j=x,y} Q_{ij}k_ik_j + \sum_{i=x,y} P_ik_i + \phi(\mathbf{k}_\parallel^{(\alpha)})\,. \end{aligned} \tag{57}$$

The expansion coefficients Q_{ij}, P_i, and $\phi(\mathbf{k}_\parallel^{(\alpha)})$ are determined by a least-square fit to values of $\phi(\mathbf{k}_\parallel)$ calculated in the vicinity of $\mathbf{k}_\parallel^{(\alpha)}$. This procedure allows to eliminate numerical inaccuracies with respect to both the values of Q_{ij} and the position of the stationary point $\mathbf{k}_\parallel^{(\alpha)}$, and it is applicable even for disordered surfaces. By inserting (56) and (57) into (55) we find

$$\begin{aligned}\mathcal{E}_x &\approx \frac{1}{\pi N V_{\mathrm{SBZ}}}\,\mathrm{Im}\left\{ g(\mathbf{k}_\parallel^{(\alpha)}) \times \right. \\ &\qquad \left. \iint_D \exp\Big[iN\Big(\phi(\mathbf{k}_\parallel^{(\alpha)}) + \sum_{i,j=x,y} Q_{ij}(k_i - k_j^{(\alpha)})(k_j - k_j^{(\alpha)})\Big)\Big]\,\mathrm{d}k_x\,\mathrm{d}k_y \right\} \\ &= \frac{\pi}{N^2 V_{\mathrm{SBZ}}}\,\mathrm{Im}\left\{ \frac{g(\mathbf{k}_\parallel^{(\alpha)})}{\sqrt{-\det|Q|}} \exp\Big[iN\phi(\mathbf{k}_\parallel^{(\alpha)})\Big] \right\}, \end{aligned} \tag{58}$$

where the two-dimensional integration region D extends to infinity, and V_{SBZ} denotes the volume of the SBZ. The second line in (58) is obtained by diagonalizing the quadratic form in the exponent (57) and by evaluating the resulting one-dimensional Gaussian-like integrals. The identification of the parameters is now straightforward, namely

$$Z_\alpha = \frac{\pi}{V_{\mathrm{SBZ}}}\,\frac{g(\mathbf{k}_\parallel^{(\alpha)})}{\sqrt{-\det|Q|}}\,, \quad Q_\alpha = \phi(\mathbf{k}_\parallel^{(\alpha)})\,. \tag{59}$$

3.4 Free-electron limit

The numerical efficiency of the present formalism offers an interesting possibility of testing model theories [1]. The simplest of such models is the free-electron model, because of a spherical Fermi surface with a single critical vector at $\mathbf{k}_\parallel = 0$ and a trivial correspondence between the value of the oscillation period and the band-filling. The free-electron model can be easily simulated by the present formalism by replacing the true metallic potentials

by flat potentials (the empty-sphere model). In this case the potential functions (3) are analytical functions of the lattice constant. For a suitable choice of the lattice constant and the position of the Fermi energy it is irrelevant what lattice and layer stacking is used, e.g., the fcc(001)-stack is the simplest choice. On the other hand such a model is free of the limitations usually adopted [1], e.g., the assumption of large spacer and magnetic slabs thicknesses, or the approximate evaluation of the energy integral for the case of finite temperatures.

3.5 Numerical illustrations

In Fig. 1 $N^2\mathcal{E}_x(N)$ is displayed as a function of the spacer thickness N for two semi-infinite Co(001) subsystems sandwiching an fcc-Cu spacer. The corresponding discrete Fourier transformation in Fig. 2 shows a pronounced short-period oscillations of 2.53 monolayers (MLs) while the long-period oscillations are suppressed in this geometry [13,14,49]. The results are insensitive to the choice of the lower and upper index in the summation in (50) provided the preasymptotic region is excluded [14].

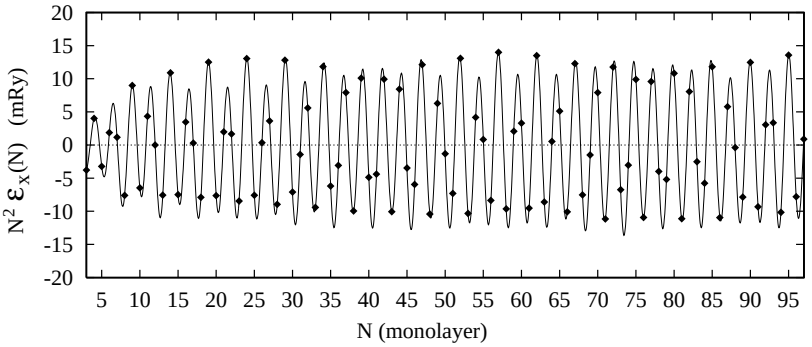

Fig. 1. Exchange coupling $N^2\mathcal{E}_x(N)$ at $T = 0$ K as a function of the spacer thickness N for two semi-infinite fcc Co(001) subsystems sandwiching a Cu spacer. Diamonds refer to the calculated values, the full line (back Fourier transform) serves as a guide to the eye

For a large enough N the IEC can be approximated by the asymptotic form in (53). The amplitude, phase, and the wave-vector entering this expression can be determined from the calculated $\mathcal{E}_x(N)$ in the manner as described in Sec. 3.2 and the asymptotic result (53) was compared with the calculated results for a large set of systems including both ideal and alloyed semi-infinite fcc(001) magnetic subsystems sandwiching a Cu-spacer: overall good agreement was found [21]. An example of the complex amplitude for this case is presented in Fig. 3 illustrating the insensitivity of the phase to elements which form the magnetic layers. It is seen that phases corresponding to Co,

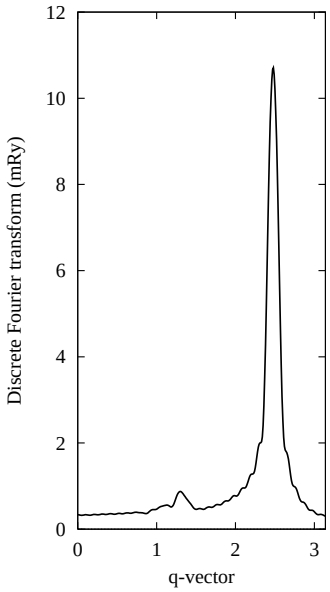

Fig. 2. Absolute value of the discrete Fourier transformation of $N^2\mathcal{E}_x(N)$ for a finite set of spacer layers (N=20–80) corresponding to two semi-infinite fcc Co(001) subsystems sandwiching a Cu spacer. The temperature is $T = 0$ K

$Fe_{50}Ni_{50}$, and $Fe_{1/3}Ni_{1/3}Co_{1/3}$ which have the same average electron numbers N_{el}=9 are nearly the same [21].

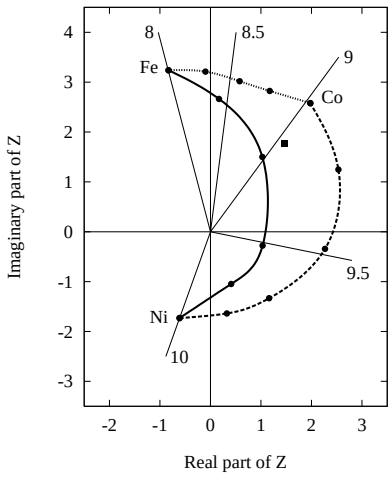

Fig. 3. Complex amplitude $Z^{1/2} = A^{1/2}\,\mathrm{e}^{i\Phi/2}$, where A and Φ are the oscillation amplitude and phase, respectively, for a semi-infinite fcc(001) subsystems formed by Fe, Co, Ni, their binary alloys (bullets), and the ternary alloy $Fe_{1/3}Co_{1/3}Ni_{1/3}$ (square) sandwiching a Cu spacer. The units are $(\mathrm{mRy})^{1/2}$. The dotted, dashed, and full lines connect various alloys and serve as a guide to the eye. The rays starting at the origin show approximately the phase corresponding to the indicated average number of valence electrons

The IEC depends on the temperature T via a factor $x/\sinh(x)$, $x = cNT$, where T is the temperature and N the spacer thickness. This remarkable result of model theories [1] was verified by calculations such as illustrated in Fig. 4.

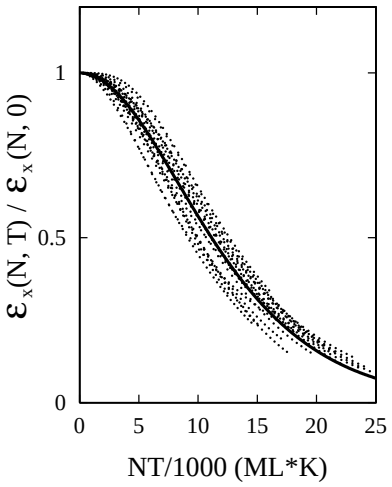

Fig. 4. $\mathcal{E}_x(N,T)/\mathcal{E}_x(N,T=0)$ plotted as a function of $\zeta = NT$ for a trilayer consisting of semi-infinite fcc Co(001)-slabs sandwiching a Cu spacer. The thick line refers to x/sinh(x), x = $c\,NT$ with $c = 0.000195$ obtained by a least square-fit to the computed data

The IEC depends in an oscillatory manner not only on the spacer thickness N but as well on the thickness P of a covering cap. The oscillations are around a biased value which corresponds to coupling for a given spacer thickness assuming a semi-infinite cap. This phenomenon is illustrated in Fig. 5 in terms of discrete Fourier transformations with respect to the spacer and the

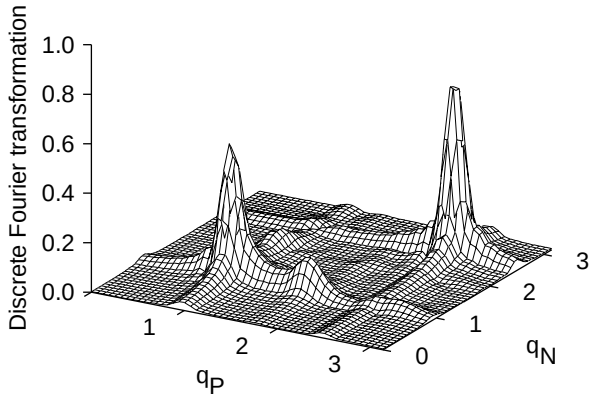

Fig. 5. Absolute values of the discrete two-dimensional Fourier transformation of $(N+P)^2\,\mathcal{E}_2(N,P)$ with respect to the spacer and the cap thickness in the case of two magnetic slabs each five monolayers thick with a Cu-substrate, a Cu-spacer, and a Cu-cap. For a definition of $\mathcal{E}_2(N,P)$ see the text

cap thickness (see Sec. 3.2) for a sample consisting of a semi-infinite fcc-Cu(001) substrate, left and right magnetic layers each five MLs thick, a spacer with varying thickness N, and a Cu-cap of varying thickness P. Fig. 5 shows:

(i) long-period oscillations (missing in Fig. 2) in addition to the short-period ones, and (ii) oscillations with respect to the cap thickness which are exactly the same as for the spacer because both are controlled by the same Fermi surface, namely that of fcc-Cu. The more complicated case of different spacer and cap materials is discussed in [23,24].

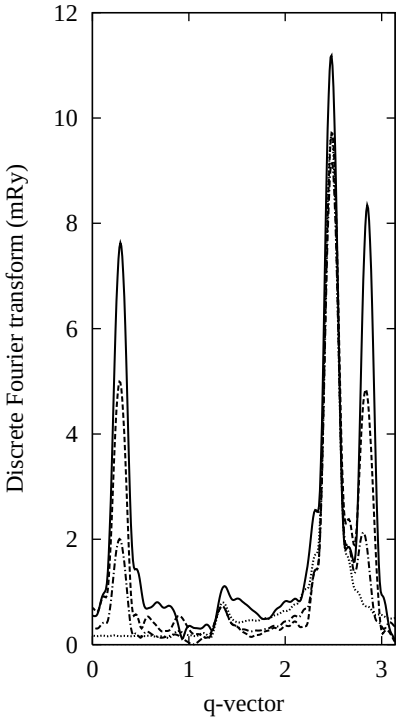

Fig. 6. Absolute values of the discrete Fourier transformation of $N^2\,\mathcal{E}_x(N)$ for two semi-infinite fcc $Co_{50}Fe_{50}(001)$ subsystems sandwiching a Cu spacer with different kinds of chemical order in magnetic layers: (**a**) $S = 1$ (complete $c(2\times 2)$-order, full line), (**b**) $S = 0.8$ (dashed line), (**c**) $S = 0.5$ (dashed-dotted line), and (**d**) $S = 0.0$ (disordered case, dotted line). The temperature is $T = 0$ K

Ordering in the spacer [22] or in the magnetic layers [20] can induce new periods due to the formation of two-dimensional sublattices. The situation is particularly interesting for a $c(2\times 2)$-ordering in magnetic layers sandwiching an ideal Cu-spacer [20]. As illustrated in Fig. 6 for full ordering two new periods with complementary periods and phases are formed in addition to a conventional short-period due to a fcc-Cu spacer [20]. These new periods vanish in the completely disordered case.

Finally, the effect of disorder in the spacer [19] is illustrated in Fig. 7. Alloying of Cu with Ni decreases the number of average valence electrons and leads to a contraction of the alloy Fermi surface, and in turn to a reduction of the coupling oscillations. The opposite behavior has to be expected for alloying of Cu with Zn, whereas only a small concentration dependence of the periods for the CuAu case is seen. The amplitudes of the oscillations are generally reduced by alloying, and in the case of CuZn spacer they are even

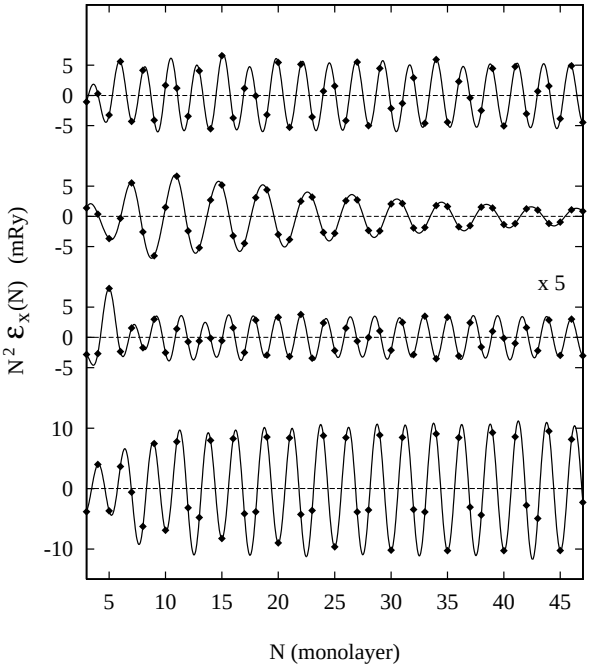

Fig. 7. Exchange coupling $N^2\mathcal{E}_x(N)$ at $T = 0$ K as a function of the spacer thickness N for two semi-infinite fcc Co(001) subsystems sandwiching a spacer of (from bottom to top) Cu, $Cu_{75}Ni_{25}$ (multiplied by a factor 5), $Cu_{50}Zn_{50}$, and $Cu_{50}Au_{50}$. Diamonds refer to the calculated values, the full line (back Fourier transform) serves as a guide to the eye

exponentially damped. The different behavior of the amplitudes can be related to differently large disorder in the neighborhood of relevant extremal points of the alloy Fermi surfaces.

3.6 List of published applications

We briefly review applications of the formalism developed in previous sections to specific problems. Additional details concerning formalism and not discussed here in details, e.g., the expansion of the IEC expression in terms of the small parameter $1 - \cos(\theta)$ or the details concerning the numerical verification of the vertex-cancellation theorem, can be found in [14,15], respectively. The influence of surface roughness (fluctuating spacer thickness and diffusion at the interface between spacer and magnetic layers) on the oscillation amplitudes was studied in [18]. The effect of alloying in the spacer [19] on the oscillation periods and their amplitudes, and in magnetic layers

[21] on the oscillation amplitudes and phases was also studied in detail for the trilayer system Co/Cu/Co(001). Ordering in disordered spacers [22] and/or magnetic [20] layers lead to a formation of new periods not present in ideal spacers. Oscillations of the IEC can originate not only due to the spacer but also from adlayers or cap layers. We refer the reader interested in this problem to a recent detailed study [23,24]. Finally, the study of the temperature dependence of the IEC and of the combined effect of the temperature and disorder is subject of very recent papers [16,17], respectively.

4 Conclusions

We have derived closed expressions for the exchange coupling between two magnetic subsystems separated by a non-magnetic spacer with a relative angle θ between the orientations of the magnetizations in the magnetic slabs. The derivation is based on a surface Green function formalism. The numerical effort scales linearly with the thickness of both the spacer and the magnetic slabs. The formulation allows also for an efficient evaluation of the temperature dependence of the coupling amplitudes. Numerical examples were chosen to illustrate the theoretical aspects rather than to give a comprehensive overview of results obtained by the present formalism or by related methods.

We wish now briefly to mention some unsolved problems. The following list is neither complete nor are the problems listed according to their importance: (i) The oscillatory dependence of the IEC on the thickness of the magnetic slabs was not yet systematically investigated on an *ab initio* level. Existing calculations [14,48,49] were performed for too thin magnetic slabs to relate occurring oscillations to extremal points of spin-polarized Fermi surfaces; (ii) The problem of biquadratic and higher order terms also did not receive a proper attention on an *ab initio* level. A relevant problem is a systematic study of situations for which the non-collinear (biquadratic) coupling can dominate. Obviously, it can happen most probably for the spacer thicknesses for which the IEC values are close to the transition between the F and AF couplings [41]. In addition, it remains to be seen whether a theoretical description of biquadratic coupling has to be based on a fully relativistic spin-polarized level; (iii) The study of superstructures in the spacer and/or in the magnetic slabs (see Sec. 2.10) offers a possibility of a deeper insight into the physical nature of the IEC because of new periods, which are connected with the extremal vectors of the spacer material in a more sophisticated manner than in the canonical cases of Cu or Cr spacers; (iv) The study of oscillatory behavior of exchange interaction across magnetic spacers is of great interest. One possibility here is to employ the method of infinitesimal rotations [9,14]; (v) The study of exchange coupling through the semiconducting or, more generally, through an insulating spacer where one expects exponential rather than N^{-2}-decay has remained limited until now to model studies [1]; (vi) The study of alloying in the spacer, magnetic layers and at interfaces

has to be extended to new interesting systems. It offers a straightforward method to obtain valuable informations concerning alloy Fermi surfaces, in particular for the case of alloyed spacers; and, finally (vii) The study of the IEC through spacers with complex Fermi surfaces, in particular through the transition metal spacers.

Acknowledgements This work is a part of activities of the Center for Computational Material Science sponsored by the Academy of Sciences of the Czech Republic. Financial support for this work was provided by the Grant Agency of the Czech Republic (Project No. 202/97/0598), the Grant Agency of the Academy Sciences of the Czech Republic (Project A1010829), the Center for the Computational Materials Science in Vienna (GZ 45.442 and GZ 45.420), and the TMR Network 'Interface Magnetism' of the European Commission (Contract No. EMRX-CT96-0089).

A Vertex cancellation theorem

We present here a general discussion of exchange interactions in the presence of substitutional disorder. The results given here are used in the present paper to study interlayer exchange interactions, but they are also applicable for studying exchange interactions within a ferromagnet, exchange stiffnesses, spin-wave energies, etc. The principal result is the "vertex cancellation theorem" of Bruno *et al.* [15]. In here we give an alternative, more general, derivation of this result.

Let $\hat{\mathbf{u}} \equiv \{\hat{\mathbf{u}}_{\mathbf{R}}\}$ be a particular configuration of the local moments, where $\hat{\mathbf{u}}_{\mathbf{R}}$ is a unit vector pointing in the direction of the $\mathbf{R}$-th local moment. We are interested in the variation of the thermodynamic grandcanonical potential

$$\Omega_{\hat{\mathbf{u}}} = -\frac{1}{\pi}\,\mathrm{Im}\int_{-\infty}^{+\infty} f(E,T)\,\mathrm{Tr}\left\langle \ln g_{\hat{\mathbf{u}}}(E+i0^{+})\right\rangle \mathrm{d}E \tag{60}$$

with respect to $\hat{\mathbf{u}}$. The Green function $g_{\hat{\mathbf{u}}}(z)$ for a particular alloy configuration is defined from the potential function $P_{\hat{\mathbf{u}}}(z)$ corresponding to $\hat{\mathbf{u}}$ as

$$g_{\hat{\mathbf{u}}}(z) = \left(P_{\hat{\mathbf{u}}}(z) - S\right)^{-1} \ . \tag{61}$$

An immediate consequence of (61) is a trivial commutator relation to be used below, namely

$$[P_{\hat{\mathbf{u}}}(z); g_{\hat{\mathbf{u}}}(z)]_{-} = [S; g_{\hat{\mathbf{u}}}(z)]_{-} \ , \tag{62}$$

where $[A;B]_{-} \equiv AB - BA$. The configuration averaged Green function $\langle g_{\hat{\mathbf{u}}}(z)\rangle \equiv \overline{g}_{\hat{\mathbf{u}}}(z)$ is usually formulated in terms of the coherent potential function $\mathcal{P}_{\hat{\mathbf{u}}}(z)$ as

$$\overline{g}_{\hat{\mathbf{u}}}(z) = \left(\mathcal{P}_{\hat{\mathbf{u}}}(z) - S\right)^{-1} \ , \tag{63}$$

which leads to a relation analogous to (62),

$$[\mathcal{P}_{\hat{\mathbf{u}}}(z); \overline{g}_{\hat{\mathbf{u}}}(z)]_- = [S; \overline{g}_{\hat{\mathbf{u}}}(z)]_- \ . \tag{64}$$

In general, the averaging in (60) cannot be reduced to $\ln \overline{g}_{\hat{\mathbf{u}}}(z)$ and an evaluation of the so-called vertex corrections is necessary. We shall show, however, that the variation of (60) due to an infinitesimal change of $\hat{\mathbf{u}}$ takes a simple form.

Let us consider the variation of the potential functions $P_{\hat{\mathbf{u}}}(z)$ in more detail. To each lattice site $\mathbf{R}$ we associate a non-random vector $\boldsymbol{\Theta}_{\mathbf{R}} \equiv \theta_{\mathbf{R}}\, \hat{\mathbf{n}}_{\mathbf{R}}$, where $\hat{\mathbf{n}}_{\mathbf{R}}$ refers to the axis of rotation and $\theta_{\mathbf{R}}$ to rotation angle by which the reference orientation $\hat{\mathbf{u}}_{0,\mathbf{R}}$ is transformed into $\hat{\mathbf{u}}_{\mathbf{R}}$. The transformed potential functions are therefore given by the following similarity transformation

$$P_{\hat{\mathbf{u}}}(z) = U_{\boldsymbol{\Theta}}\, P_{\hat{\mathbf{u}}_0}(z)\, U_{\boldsymbol{\Theta}}^{-1} \ , \tag{65}$$

where the rotation matrix $U_{\boldsymbol{\Theta}}$ in (65) is defined as

$$(U_{\boldsymbol{\Theta}})_{\mathbf{R}Ls,\mathbf{R}'L's'} = \delta_{\mathbf{R},\mathbf{R}'}\, \delta_{L,L'} \times \left[\cos\left(\frac{\theta_{\mathbf{R}}}{2}\right) \mathbb{1} \ - \ i \, \sin\left(\frac{\theta_{\mathbf{R}}}{2}\right) \hat{\mathbf{n}}_{\mathbf{R}} \cdot \boldsymbol{\sigma}\right]_{s,s'} \ . \tag{66}$$

The symbol $\boldsymbol{\sigma}$ in (66) denotes the vector of the standard 2×2 Pauli matrices and $\mathbb{1}$ is the 2×2 unit matrix. The first-order change of $P_{\hat{\mathbf{u}},\mathbf{R}}(z)$ caused by an additional infinitesimal rotation $\delta\mathbf{v}_{\mathbf{R}}$ is then expressed as

$$\delta P_{\hat{\mathbf{u}}}(z) = [\delta K; P_{\hat{\mathbf{u}}}(z)]_- \ , \tag{67}$$

where the matrix elements of the operator $\delta K = U_{\delta\mathbf{v}} - 1$ are explicitly given by

$$(\delta K)_{\mathbf{R}Ls,\mathbf{R}'L's'} = \delta_{\mathbf{R},\mathbf{R}'}\, \delta_{L,L'}\, \frac{(-i)}{2}\, [\boldsymbol{\sigma} \cdot \delta\mathbf{v}_{\mathbf{R}}]_{s,s'} \ . \tag{68}$$

The introduced infinitesimal rotation vectors $\delta\mathbf{v}_{\mathbf{R}}$ satisfy $U_{\delta\mathbf{v}}\, U_{\boldsymbol{\Theta}} = U_{\boldsymbol{\Theta}+\delta\boldsymbol{\Theta}}$ whereas, in general, $U_{\delta\boldsymbol{\Theta}}\, U_{\boldsymbol{\Theta}} \neq U_{\boldsymbol{\Theta}+\delta\boldsymbol{\Theta}}$. Let us note that δK is a non-random site-diagonal operator.

The first-order variation of $\mathrm{Tr}\,\langle \ln g_{\hat{\mathbf{u}}}(z)\rangle$ can be now formulated using (94, 67) as

$$\delta \mathrm{Tr}\,\langle \ln g_{\hat{\mathbf{u}}}(z)\rangle = -\,\mathrm{Tr}\,\big\langle g_{\hat{\mathbf{u}}}(z)\ [\delta K; P_{\hat{\mathbf{u}}}(z)]_-\big\rangle \ , \tag{69}$$

which can be rewritten by applying the permutation invariance of the trace and (62, 64) as

$$\begin{aligned}
\delta \mathrm{Tr}\,\langle \ln g_{\hat{\mathbf{u}}}(z)\rangle &= -\,\mathrm{Tr}\,\big\{\delta K\ \big\langle [P_{\hat{\mathbf{u}}}(z); g_{\hat{\mathbf{u}}}(z)]_-\big\rangle\big\} \\
&= -\,\mathrm{Tr}\,\big\{\delta K\ \big\langle [S; g_{\hat{\mathbf{u}}}(z)]_-\big\rangle\big\} \\
&= -\,\mathrm{Tr}\,\big\{\delta K\ [S; \overline{g}_{\hat{\mathbf{u}}}(z)]_-\big\} \\
&= -\,\mathrm{Tr}\,\big\{\delta K\ [\mathcal{P}_{\hat{\mathbf{u}}}(z); \overline{g}_{\hat{\mathbf{u}}}(z)]_-\big\} \ .
\end{aligned} \tag{70}$$

By using the permutation invariance of the trace once again, (70) can be given the final form

$$\delta \mathrm{Tr}\, \langle \ln g_{\hat{\mathbf{u}}}(z) \rangle = -\,\mathrm{Tr}\, \left\{ \overline{g}_{\hat{\mathbf{u}}}(z)\, [\delta K; \mathcal{P}_{\hat{\mathbf{u}}}(z)]_- \right\} \ . \tag{71}$$

Let us note that (71) was derived in a formally exact alloy theory, but is valid in the CPA as well. Within the CPA, the result (71) has an obvious interpretation: the r.h.s. describes the variation of $\mathrm{Tr} \ln \overline{g}_{\hat{\mathbf{u}}}(z)$ induced by performing on the site-diagonal coherent potential functions $\mathcal{P}_{\hat{\mathbf{u}},\mathbf{R}}(z)$ the same rotations (68) as applied to the potential functions $P_{\hat{\mathbf{u}},\mathbf{R}}(z)$; note however, that this is *not* equal to the infinitesimal change of the true *self-consistent* CPA coherent potential function.

Thus, the torque acting on the moment at site $\mathbf{R}$ due to the exchange interactions is given by

$$\begin{aligned} \boldsymbol{\Gamma}_{\hat{\mathbf{u}},\mathbf{R}} \equiv -\frac{\delta \Omega_{\hat{\mathbf{u}}}}{\delta \mathbf{v}_{\mathbf{R}}} = -\frac{1}{\pi} \int_{-\infty}^{+\infty} f(E,T) \times \\ \mathrm{Im}\ \mathrm{Tr} \left\{ \overline{g}_{\hat{\mathbf{u}}}(E+i0^+)\, \frac{(-i)}{2}\, \left[\Pi_{\mathbf{R}}\, \boldsymbol{\sigma}\, ;\, \mathcal{P}_{\hat{\mathbf{u}}}(E+i0^+) \right]_- \right\} \mathrm{d}E \ , \end{aligned} \tag{72}$$

where $\Pi_{\mathbf{R}}$ is a projector on site $\mathbf{R}$. This exact result constitutes the "vertex cancellation theorem" for the torque. Its usefulness arises from the fact that the "vertex corrections" have been eliminated.

In order to compute the difference of thermodynamic grandcanonical potential between two local moment configurations $\hat{\mathbf{u}}_1$ and $\hat{\mathbf{u}}_2$ in the CPA, we use a theorem due to Ducastelle [31], which states that the thermodynamic grandcanonical potential, considered as a functional $\tilde{\Omega}[\mathcal{P}, P]$ of the independent variables $\mathcal{P}$ and P, is stationary with respect to $\mathcal{P}$ when the latter satisfies the CPA self-consistency condition. This means that a first-order error in $\mathcal{P}_{\hat{\mathbf{u}}}$ gives only a second-order error in $\Omega_{\hat{\mathbf{u}}}$. Let us approximate $\mathcal{P}_{\hat{\mathbf{u}}}(z)$ by

$$\mathcal{P}_{\hat{\mathbf{u}}}(z) \approx \mathcal{P}'_{\hat{\mathbf{u}}}(z) \equiv U_{\boldsymbol{\Theta}}\, \mathcal{P}_{\hat{\mathbf{u}}_0}(z)\, U_{\boldsymbol{\Theta}}^{-1} \ , \tag{73}$$

i.e., we assume that $\mathcal{P}_{\hat{\mathbf{u}}}(z)$ is transformed like $P_{\hat{\mathbf{u}}}(z)$ under a rotation of the local moment direction. This can be expected to be a good approximation, provided the condition

$$m_{\mathbf{R}} \left| \frac{\mathrm{d}\boldsymbol{\Theta}_{\mathbf{R}}}{\mathrm{d}\mathbf{R}} \right| \ll k_F\, q_{\mathbf{R}} \tag{74}$$

is satisfied, where $q_{\mathbf{R}}$ and $m_{\mathbf{R}}$ are respectively the charge and spin moment at site $\mathbf{R}$. We then get

$$\overline{g}_{\hat{\mathbf{u}}}(z) \approx \overline{g}'_{\hat{\mathbf{u}}}(z) \equiv \left(\mathcal{P}'_{\hat{\mathbf{u}}}(z) - S \right)^{-1} . \tag{75}$$

Replacing $\mathcal{P}_{\hat{\mathbf{u}}}$ by $\mathcal{P}'_{\hat{\mathbf{u}}}$ and $\overline{g}_{\hat{\mathbf{u}}}$ by $\overline{g}'_{\hat{\mathbf{u}}}$ in (71), we obtain

$$\delta \mathrm{Tr}\, \langle \ln g_{\hat{\mathbf{u}}}(z) \rangle \approx \delta \mathrm{Tr}\, \ln \overline{g}'_{\hat{\mathbf{u}}}(z) \ , \tag{76}$$

and integrating over the angles, we get

$$\Omega_{\hat{\mathbf{u}}_1} - \Omega_{\hat{\mathbf{u}}_2} \approx -\frac{1}{\pi}\int_{-\infty}^{+\infty} f(E,T) \times \\ \mathrm{Im\ Tr}\left[\ln \overline{g}'_{\hat{\mathbf{u}}_1}(E+\mathrm{i}0^+) - \ln \overline{g}'_{\hat{\mathbf{u}}_2}(E+\mathrm{i}0^+)\right] \mathrm{d}E \ , \tag{77}$$

which constitutes the "vertex cancellation theorem" for exchange energies. Note that we have derived here a form of the "vertex cancellation theorem" within the CPA since this is the scheme which is used in practical calculations; however, one can prove that the same result holds if one takes the exact solution to the configuration averaging problem.

In the case of interlayer coupling, the condition (74) is satisfied even for large rotation angles, because $\mathrm{d}\boldsymbol{\Theta}_{\mathbf{R}}/\mathrm{d}\mathbf{R}$ differs from zero only in a region where $m_{\mathbf{R}}$ is negligible. This was confirmed by explicit numerical calculations in [15].

B The interface-interface part of the grandcanonical potential

In this Appendix we derive the basic relations for an evaluation of the IEC within the interface-interface interaction formulation.

The subsystems $\mathcal{L}$ and $\mathcal{R}$ can be downfolded using the formula (88)

$$\begin{aligned} &\mathrm{Tr}\ln(P-S) = \mathrm{Tr}_{\mathcal{L}}\ln\Big[P-S\Big] + \mathrm{Tr}_{\mathcal{R}}\ln\Big[P-S\Big] \\ &+ \mathrm{Tr}_{\mathcal{C}}\ln\Big[(P-S)_{\mathcal{C}\mathcal{C}} - (P-S)_{\mathcal{C}\mathcal{L}}\frac{\mathcal{L}}{P-S}(P-S)_{\mathcal{L}\mathcal{C}} \\ &- (P-S)_{\mathcal{C}\mathcal{R}}\frac{\mathcal{R}}{P-S}(P-S)_{\mathcal{R}\mathcal{C}}\Big]. \end{aligned} \tag{78}$$

The first two terms are independent of the rotation angle θ and, consequently, they do not contribute to the exchange energy $\mathcal{E}_x(\theta)$. We are thus left with a quantity which is limited to the subspace $\mathcal{C}$ only. It is now easy to identify the individual terms in (78). The potential function blocks between different subspaces such as $P_{\mathcal{L}\mathcal{C}}$ or $P_{\mathcal{C}\mathcal{R}}$ are zero because the potential function P is site-diagonal. The blocks of S between neighboring subspaces do not vanish, but the non-zero subblocks connect only neighboring principal layers. The important part of the $\mathrm{Tr}\ln(P-S)$ is then reduced to

$$\mathrm{Tr}_{\mathcal{C}}\ln(P-S)_{\mathcal{C}\mathcal{C}} + \mathrm{Tr}_{\mathcal{C}}\ln\Big[1 - \frac{\mathcal{C}}{P-S}S_{10}\mathcal{G}_{\mathcal{L}}S_{01} - \frac{\mathcal{C}}{P-S}S_{01}\mathcal{G}_{\mathcal{R}}S_{10}\Big]. \tag{79}$$

The first term is independent of θ and thus does not contribute to the exchange energy. The second term can be simplified using the two-potential formula (93). We identify $G^{(0)} = \mathcal{C}/(P-S)$, $v_1 = S_{10}\mathcal{G}_{\mathcal{L}}S_{01}$, and $v_2 = S_{01}\mathcal{G}_{\mathcal{R}}S_{10}$. The t-matrices are then identical with the τ-matrices, and the potentials v_1

and v_2 are equal to the embedding potentials Γ_1 and Γ_2. In this way we find the expression for the grandcanonical potential

$$\Omega(\theta,T,\mu) = \Omega_0(T,\mu)$$
$$-\frac{1}{\pi}\,\mathrm{Im}\int_{-\infty}^{\infty} f(E,T,\mu)\,\mathrm{Tr}_1 \ln\left[1-g_{1N}(z)\tau_N(z)g_{N1}(z)\tau_1(z)\right]dz\,, \qquad (80)$$

where $\Omega_0(T,\mu)$ contains all the terms independent of θ and the Tr_1 applies only to the layer 1, i.e., the first spacer layer. If the system is invariant with respect to translations in the planes of atoms, or, if such a symmetry is restored by configuration averaging, (80) can be written as

$$\Omega(\theta,T,\mu) = \Omega_0(T,\mu) - \frac{1}{\pi}\,\mathrm{Im}\int_{-\infty}^{\infty} f(E,T,\mu)\times$$
$$\sum_{\mathbf{k}_{||}} \mathrm{tr}\ln\left[1-g_{1N}(\mathbf{k}_\parallel,z)\tau_N(\mathbf{k}_\parallel,z)g_{N1}(\mathbf{k}_\parallel,z)\tau_1(\mathbf{k}_\parallel,z)\right]dz\,, \qquad (81)$$

where tr means the trace over angular momentum indices $L=(\ell m)$ and the spin index σ.

C Useful mathematical tools

Theoretical developments and many calculations are facilitated by the partitioning technique and the two-potential formula applied to the Green function and its logarithm.

Let P and Q denote projection operators onto the complementary subspaces (i.e. $P+Q=1$). We denote the projections of matrices as $PAP = A_{PP}, PAQ = A_{PQ}$, etc., and P/A means the inversion of A_{PP} in the subspace referring to projector P. In most applications, $A = z - H$ or $A = P(z) - S$ and $G(z) = A^{-1}$.

The projections of the inverse A^{-1} to the matrix A are given by [50]

$$(A^{-1})_{PP} = \frac{P}{A_{PP} - A_{PQ}\frac{Q}{A}A_{QP}}\,, \qquad (82)$$

$$(A^{-1})_{QQ} = \frac{Q}{A_{QQ} - A_{QP}\frac{P}{A}A_{PQ}}\,, \qquad (83)$$

$$(A^{-1})_{PQ} = -\frac{P}{A}A_{PQ}(A^{-1})_{QQ} = -(A^{-1})_{PP}A_{PQ}\frac{Q}{A}\,, \qquad (84)$$

$$(A^{-1})_{QP} = -\frac{Q}{A}A_{QP}(A^{-1})_{PP} = -(A^{-1})_{QQ}A_{QP}\frac{P}{A}\,. \qquad (85)$$

It is sometimes easier to invert the full matrix A than its blocks. In such a case the inverse partitioning is useful

$$\frac{P}{A_{PP}} = (A^{-1})_{PP}\frac{P}{P - A_{PQ}(A^{-1})_{QP}} = \frac{P}{P-(A^{-1})_{PQ}A_{QP}}(A^{-1})_{PP}\,. \qquad (86)$$

This can be used to calculate the surface Green function of a semi-infinite system from the Green function of the infinite system.

Partitioning technique also allows to simplify calculations involving Tr ln of a matrix. The basic relation is

$$\mathrm{Tr}\ln A = \ln\det A\,. \tag{87}$$

It then follows $\mathrm{Tr}\ln AB = \mathrm{Tr}\ln A + \mathrm{Tr}\ln B$, $\mathrm{Tr}\ln 1 = 0$, $\mathrm{Tr}\ln(A^{-1}) = -\mathrm{Tr}\ln A$, and $\mathrm{Tr}\ln[(A-B)^{-1}] = -\mathrm{Tr}\ln A - \mathrm{Tr}\ln[1-A^{-1}B]$. The Tr ln A can then be partitioned as

$$\mathrm{Tr}\ln A = \mathrm{Tr}_P \ln[PAP] + \mathrm{Tr}_Q \ln[QAQ - QA\frac{P}{A}AQ]. \tag{88}$$

To prove (88), let us multiply the matrix A by $L = 1 - A_{QP}(P/A)$ from left and by $R = 1 - (P/A)A_{PQ}$ from right. The result is $LAR = A_{PP} + A_{QQ} - A_{QP}(P/A)A_{PQ}$. Now using (87), and the fact that $\det[L] = \det[R] = 1$ we find (88). In a special, but important case, when $A_{PP} = P$ and $A_{QQ} = Q$ it holds

$$\begin{aligned}\mathrm{Tr}\ln A &= \mathrm{Tr}_{P+Q}\ln[P+Q+A_{PQ}+A_{QP}] \\ &= \mathrm{Tr}_P\ln[P-A_{PQ}A_{QP}] = \mathrm{Tr}_Q\ln[Q-A_{QP}A_{PQ}]\,.\end{aligned} \tag{89}$$

The Green function of a system described by the Hamiltonian $H = H_0 + v_1 + v_2$, where H_0 is the unperturbed part, and $v_i (i = 1, 2)$ are perturbing potentials, is given by $G = G^{(0)} + G^{(0)}TG^{(0)}$, where $G = (z - H)^{-1}$, $G^{(0)} = (z - H_0)^{-1}$, and $T = V(1 - G^{(0)}V)^{-1}$, where $V = v_1 + v_2$. The full T-matrix T can be expressed in terms of the t-matrices, $t_i = v_i(1 - G^{(0)}v_i)^{-1}, (i = 1, 2)$ and of the unperturbed resolvent $G^{(0)}$ by the the two-potential formula

$$\begin{aligned}T = {} & t_1\left[1 - G^{(0)}t_2G^{(0)}t_1\right]^{-1}\left(1 + G^{(0)}t_2\right) + t_2\left[1 - G^{(0)}t_1G^{(0)}t_2\right]^{-1} \times \\ & \left(1 + G^{(0)}t_1\right).\end{aligned} \tag{90}$$

It is derived in the following way. Because

$$(1-A)[1-(1-A)^{-1}AB(1-B)^{-1}](1-B) = 1 - A - B\,, \tag{91}$$

it holds

$$\begin{aligned}\mathrm{Tr}\ln[1-A-B] &= \mathrm{Tr}\ln[1-A] + \mathrm{Tr}\ln[1-B] \\ &\quad + \mathrm{Tr}\ln\left[1-(1-A)^{-1}AB(1-B)^{-1}\right].\end{aligned} \tag{92}$$

By inserting $A = G^{(0)}v_1$ and $B = G^{(0)}v_2$ into (92) one obtains (90). The two-potential formula for the Tr ln of the full Green function

$$\begin{aligned}\mathrm{Tr}\ln G &= \mathrm{Tr}\ln G^{(0)}[1 - VG^{(0)}]^{-1} \\ &= \mathrm{Tr}\ln G^{(0)} - \mathrm{Tr}\ln[1 - G^{(0)}v_1 - G^{(0)}v_2] \\ &= \mathrm{Tr}\ln G^{(0)} - \mathrm{Tr}\ln[1 - G^{(0)}v_1] - \mathrm{Tr}\ln[1 - G^{(0)}v_2] \\ &\quad -\mathrm{Tr}\ln[1 - G^{(0)}t_1G^{(0)}t_2]\end{aligned} \tag{93}$$

follows directly from (92).

If the matrix A is a function of a variable z (complex in the general case), the derivative with respect to z is given by

$$\frac{d}{dz}\mathrm{Tr}\ln\left[A(z)\right] = \mathrm{Tr}\left[\frac{d}{dz}A(z)\,A^{-1}(z)\right], \tag{94}$$

provided that the matrix $A(z)$ is nonsingular. This identity is used to derive the expression of the grandcanonical potential Ω in terms of the auxiliary Green function (12) within the TB-LMTO.

The identity in (87) is valid up to an integer multiple of $2\pi i$. Neglecting this fact can lead to serious errors. There is no panacea for this kind of difficulties, but in some situations they can be avoided, for example by choosing the integration contour parallel to the imaginary axis, but this is not always possible. In some cases the incremental procedure for calculating the ln det, $\ln f(z_{k+1}) = \ln f(z_k) + \ln\left[f(z_{k+1})/f(z_k)\right]$ in the spirit of an analytical continuation can be helpful, provided that the change of phase between two consecutive points z_k is less than 2π. To insure this, one has to choose a sufficiently small grid in z.

D Inversion of block-tridiagonal matrices

We wish to compute $g = A^{-1}$ for a block-tridiagonal A. The matrix A is divided into $N \times N$ square subblocks of the same dimension m, from which non-zero are only $A_{k,k}$, $A_{k-1,k}$, and $A_{k,k-1}$. The diagonal blocks are a sum of two terms: hermitean matrix and a symmetric complex matrix. They are always non-singular. The off-diagonal blocks under the diagonal are equal to hermitean conjugate of the corresponding blocks above the diagonal ($A_{k,k-1} = A^{+}_{k-1,k}$). The methods based on repeated use of partitioning are particularly efficient if only diagonal blocks, or four so-called 'corner' blocks ($g_{1,1}, g_{N,N}, g_{1,N}, g_{N,1}$) are needed like in the interlayer exchange coupling calculations.

First, four sequences of auxiliary matrices are calculated

$$\begin{aligned}
X_{N-k} &= A_{N-k,N-k+1}(A_{N-k+1,N-k+1} - X_{N-k+1})^{-1}A_{N-k+1,N-k}\,, \\
X_N &= 0, \quad (k = 1, \ldots N-1)\,, \\
Y_{k+1} &= A_{k+1,k}(A_{k,k} - Y_k)^{-1}A_{k,k+1}\,, \quad Y_1 = 0, \quad (k = 2, \ldots N) \\
Z_k &= -(A_{k,k} - X_k)^{-1}A_{k,k-1}, \quad (k = 2, \ldots N) \\
W_k &= -(A_{k,k} - Y_k)^{-1}A_{k,k+1}, \quad (k = 1, \ldots N-1)\,,
\end{aligned} \tag{95}$$

that are used to compute the diagonal and off-diagonal blocks of g

$$\begin{aligned}
g_{k,k} &= (A_{k,k} - X_k - Y_k)^{-1}\,, \\
g_{i,j} &= Z_i\, g_{i-1,j} \quad \text{for} \quad i > j\,, \\
g_{i,j} &= W_i\, g_{i+1,j} \quad \text{for} \quad i < j\,.
\end{aligned} \tag{96}$$

It can be proved that the numerical effort to evaluate the corner blocks scales as $O(Nm^3)$. The details, particularly the tests of efficiency can be found in [42].

References

1. P. Bruno, Phys. Rev. B **52**, 411 (1995).
2. J. Mathon, M. Villeret, A. Umerski, R.B. Muniz, J. d'Albuquerque e Castro, and D.M. Edwards, Phys. Rev. B **56**, 11797 (1997).
3. See theoretical and experimental review articles in IBM J. Res. Development **42**, No. 1 (1998).
4. M. van Schilfgaarde, F. Herman, S.S.P. Parkin, and J. Kudrnovský, Phys. Rev. Lett. **74**, 4063 (1995).
5. M. van Schilfgaarde and F. Herman, Phys. Rev. Lett. **71**, 1923 (1993).
6. S. Mirbt, H.L. Skriver, M. Aldén, and B. Johansson, Solid State Commun. **88**, 331 (1993).
7. M.D. Stiles, Phys. Rev. B **48**, 7238 (1993).
8. A. Oswald, R. Zeller, P.J. Braspenning, and P.H. Dederichs, J. Phys. F: Met. Phys. **15**, 193 (1985).
9. A.I. Liechtenstein, M.I. Katsnelson, V.P. Antropov, and V.A. Gubanov, J. Magn. Magn. Mater. **67**, 65 (1987).
10. A.R. Mackintosh and O.K. Andersen, in *Electrons at the Fermi Surface*, Ch. 5.3., ed. M. Springford (Cambridge University Press, Cambridge, England, 1980).
11. P. Lloyd and P.V. Smith, Adv. Phys. **21**, 69 (1972).
12. P. Lang, L. Nordström, R. Zeller, and P.H. Dederichs, Phys. Rev. Lett. **71**, 1927 (1993).
13. J. Kudrnovský, V. Drchal, I. Turek, and P. Weinberger, Phys. Rev. B **50**, 16105 (1994).
14. V. Drchal, J. Kudrnovský, I. Turek, and P. Weinberger, Phys. Rev. B **53**, 15036 (1996).
15. P. Bruno, J. Kudrnovský, V. Drchal, and I. Turek, Phys. Rev. Lett. **76**, 4254 (1996).
16. V. Drchal, J. Kudrnovský, P. Bruno, and P. Weinberger, Phil. Mag. B **78**, 571 (1998).
17. V. Drchal, J. Kudrnovský, P. Bruno, P.H. Dederichs, and P. Weinberger, (to be submitted).
18. J. Kudrnovský, V. Drchal, I. Turek, M. Šob, and P. Weinberger, Phys. Rev. B **53**, 5125 (1996).
19. J. Kudrnovský, V. Drchal, P. Bruno, I. Turek, and P. Weinberger, Phys. Rev. B **54**, R3738 (1996).
20. J. Kudrnovský, V. Drchal, C. Blass, I. Turek, and P. Weinberger, Phys. Rev. Lett. **76**, 3834 (1996).
21. J. Kudrnovský, V. Drchal, R. Coehoorn, M. Šob, and P. Weinberger, Phys. Rev. Lett. **78**, 358 (1997).
22. P. Bruno, J. Kudrnovský, V. Drchal, and I. Turek, J. Magn. Magn. Mater. **165**, 128 (1997).

23. J. Kudrnovský, V. Drchal, P. Bruno, I. Turek, and P. Weinberger, Phys. Rev. B **56**, 8919 (1997).
24. J. Kudrnovský, V. Drchal, P. Bruno, R. Coehoorn, J.J. de Vries, K. Wildberger, P.H. Dederichs, and P. Weinberger, MRS Symposium Proceedings, eds. J. Tolbin et al., Vol. **475**, 575 (1997).
25. O.K. Andersen and O. Jepsen, Phys. Rev. Lett. **53**, 2571 (1984).
26. I. Turek, V. Drchal, J. Kudrnovský, M. Šob, and P. Weinberger, *Electronic Structure of Disordered Alloys, Surfaces and Interfaces* (Kluwer, Boston-London-Dordrecht, 1997)
27. See I. Turek, J. Kudrnovský, and V. Drchal, these Proceedings.
28. V. Drchal, J. Kudrnovský, L. Udvardi, P. Weinberger, and A. Pasturel, Phys. Rev. B **45**, 14328 (1992).
29. See, for example, A. Messiah, *Quantum Mechanics*, vol. II, (North-Holland, Amsterdam, 1969), Appendix C.
30. P. Lang, L. Nördstrom, K. Wildberger, R. Zeller, and P.H. Dederichs, Phys. Rev. B **53**, 9092 (1996).
31. F. Ducastelle, J. Phys. C: Solid State Phys. **8**, 3297 (1975).
32. L. Szunyogh, B. Újfalussy, P. Weinberger, and C. Sommers, Phys. Rev. B **54**, 6430 (1996).
33. B. Wenzien, J. Kudrnovský, V. Drchal, and M. Šob, J. Phys.: Condens. Matter **1**, 9893 (1989).
34. J. Kudrnovský, I. Turek, V. Drchal, P. Weinberger, N.E. Christensen, and S.K. Bose, Phys. Rev. B **46**, 4222 (1992).
35. J. Kudrnovský, I. Turek, V. Drchal, P. Weinberger, S.K. Bose, and A. Pasturel, Phys. Rev. B **47**, 16525 (1993).
36. V. Drchal, J. Kudrnovský, and I. Turek, Comp. Phys. Commun. **97**, 111 (1996).
37. P. Weinberger, Phil. Mag. B **75**, 509 (1997).
38. J. Zabloudil, C. Uiberacker, U. Pustogowa, B. Blaas, L. Szunyogh, C. Sommers, and P. Weinberger, Phys. Rev. B **57**, 7804 (1998).
39. J.C. Slonczewski, Phys. Rev. B **39**, 6995 (1989).
40. D.M. Edwards, A.M. Robinson, and J. Mathon, J. Mag. Mag. Mat. **140-144**, 517 (1995).
41. C. Blaas, P. Weinberger, L. Szunyogh, J. Kudrnovský, V. Drchal, P.M. Levy, and C. Sommers (submitted to J. Phys. I France).
42. E.M. Godfrin, J. Phys.: Condens. Matter **3**, 7843 (1991).
43. P. Weinberger, I. Turek, and L. Szunyogh, Int. J. Quant. Chem. **63**, 165 (1997).
44. M.S. Ferreira, J. Phys. Condens. Matter **9**, 6665 (1997).
45. J. d'Albuquerque e Castro, J. Mathon, M. Villeret, and A. Umerski, Phys. Rev. B **53**, R13306 (1996).
46. C. Lanczos, *Applied Analysis*, (Dover, New York, 1988), p. 219.
47. P. Bruno, J. Magn. Magn. Mater. **164**, 27 (1996).
48. S. Krompiewski, F. Süss, and U. Krey, Europhys. Lett. **26**, 303 (1994).
49. L. Nördstrom, P. Lang, R. Zeller, and P.H. Dederichs, Phys. Rev. B **50**, 13058 (1994).
50. P.O. Löwdin, J. Chem. Phys. **19**, 1396 (1951).